An FCN-based approach to analyse dynamics of urbanizing areas

XUJIAYI YANG
June 2020

SUPERVISORS:
Prof. dr. K. Pfeffer
Dr. M. Kuffer
Dr. C. Persello

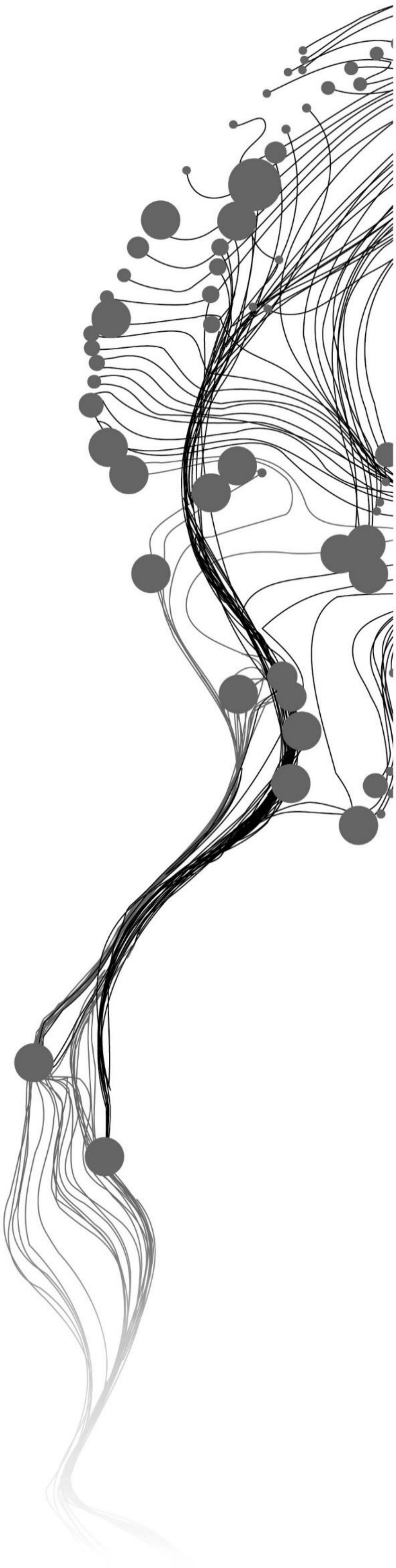

An FCN-based approach to analyse dynamics of urbanizing areas

XUJIAYI YANG
Enschede, The Netherlands, June 2020

Thesis submitted to the Faculty of Geo-Information Science and Earth Observation of the University of Twente in partial fulfilment of the requirements for the degree of Master of Science in Geo-information Science and Earth Observation.
Specialization: Urban Planning and Management

SUPERVISORS:
Prof. dr. K. Pfeffer
Dr. M. Kuffer
Dr. C. Persello

THESIS ASSESSMENT BOARD:
[Prof.dr. R.V. Sliuzas (Chair)]
[Dr. M. Wurm (External Examiner, German Aerospace Centre (DLR))]
etc

ABSTRACT

Urbanization rates are accelerating considerably in recent years. Presently, research on urbanization dynamics mainly focuses on large cities, while small urbanizations are not well covered. Also, not much data is available on urbanization processes in small urbanizing areas. For example, global datasets on built-up areas often omit small urbanizations. Remote sensing images are increasingly used for the spatial analysis of the dynamics of urban areas and could fill this information gap. Such data combined with machine learning algorithms such as fully convolutional networks (FCN) can classify land cover/use classes from satellite images and further extract contiguous built-up areas. Although there are projects that manually delineate contiguous built-up areas, they are time-consuming and labour-intensive. The objective of this study is to develop an FCN-based approach to semi-automatically delineate and analyse the spatial dynamics of urbanizing areas. It uses the example of the Barharia cluster, a small region located in the Bihar state of India, which consists of six villages. This study regards contiguous built-up areas with more than 10,000 people as urbanizing areas. To delineate urbanizing areas, this study takes advantages of deep learning and applied FCN with dilated kernels to classify built-up areas, roads and non-built-up areas from very high resolution (VHR) images in 2005, 2010 and 2018. The contiguous built-up areas were derived by aggregating classified built-up areas with a gap of less than 200 metres. Meanwhile, the population of each contiguous built-up area was estimated based on the census data of Bihar in 2001 and 2011, and the administrative boundaries of settlements in the study area. Finally, spatial metrics was used to analyse the dynamics of urbanizing areas. The classification accuracy of built-up areas in all three years obtained a F1-score of more than 84%. Based on the used definition, one urbanizing area was identified respectively in 2010 and 2018, and there was no urbanizing area in this study area in 2005. Results of spatial metrics calculation indicated that contiguous built-up areas aggregated over time and the urbanizing areas expanded from 2010 to 2018. Moreover, the population density of urbanizing areas decreased from 2010 to 2018 and the land use efficiency of this study area was also decreased over time. This study concludes that the developed FCN-based approach can delineate urbanizing areas in a semi-automatic manner, and based on the analysis of the classification results, expanding urbanizing areas (from 137.44 ha in 2010 to 314.62 ha in 2018) were found in the study area. However, in the developed approach, the assumption made for population estimation and census data disaggregation is quite simple. Nevertheless, the method used for contiguous built-up area extraction is more time-efficient than manual delineation. This shows a potential to develop approaches for the efficient delineation and spatial dynamic analysis of urbanizing areas in small regions.

Keywords: urbanizing area delineation, very high resolution (VHR) satellite imagery, fully convolutional networks (FCN), population estimation

ACKNOWLEDGEMENTS

I would like to express my deepest gratitude to my supervisors, Prof. dr. K. Pfeffer and Dr. M. Kuffer, as well as my advisor Dr. C. Persello. Their suggestions and ideas prompted me to continuously improve my MSc research. Their encouragement and enthusiasm also made me feel more confident when facing difficulties. I would also express my thanks to Dr. candidate R.J. Van Duijne for sharing the information obtained during his fieldwork in India.

I would like to acknowledge the support of the European Space Agency (ESA) for approving the proposal numbered 55572 and providing VHR images of the study area for free. I also want to express my gratitude to P.E. Budde from the Remote Sensing and GIS lab in ITC. She provided me suggestions on the selection and pre-processing of satellite images.

I would like to thank all my friends in the Netherlands. They accompanied me a very pleasant study life and made me feel at home. They always provided me selfless help when I got trouble.

Last but not least, I would like to express my appreciation to my family. They provided me great support during my stay in the Netherlands and kept encouraging me to pursue the life I want.

TABLE OF CONTENTS

LIST OF FIGURES

LIST OF TABLES

1. INTRODUCTION

1.1. Background justification

Driven by rapid economic development and population growth, the extent of urban areas and contiguous built-up areas have grown significantly over the past two decades. As reported by the United Nations (2018), the proportion of the urban population was estimated at 55.3% in 2018 and is expected to increase to 60% in 2030. Generating spatial information about the urbanization process can help visualizing urban development patterns and inform urban planners to formulate targeted policies with the ambition to build resilient and sustainable cities, laid down in Goal 11 of the Sustainable Development Goals (SDGs) by the United Nations (2015).

Urbanization refers to the increasing percentage of dwellers living in urban areas compared to the total number of residents (Tacoli, Gordon, & David, 2015). There are various driving forces of urbanization and one of them is economic growth. For example, industrial corridors constructed in many countries like India link big cities and towns via transport axes and promoting economic developments, therefore stimulating the urbanization process of regions along the industrial corridors (Ramachandra, Sellers, Bharath, & Vinay, 2019). The transformation from farm works to non-farm works in some rural areas and the rural-urban circular migration are also driving forces of urbanization and mainly cause in situ urbanization in countries like China, Indonesia, and India (Champion, Hugo, & Zhu, 2018; Van Duijne & Nijman, 2019). These factors may increase the income of residents in rural-urban transition areas and result in the emergence of urban development at the place where they live. Denis, Mukhopadhyay and Zérah (2017) also introduced a concept of 'subaltern urbanisation', focusing on the urbanization process of small areas where vigorous social and economic activities mainly happened within the region.

The definition of urban differs among countries and projects related to urban development research. These definitions are further elaborated in section 2.1. Most countries define urban according to the population size or together with some other criteria like economic activities (United Nations, 2017). However, the determination of urban areas should not only be constraint to official administrative city boundaries, but also include urbanizing areas that have distinct differences as compared to non-urbanizing areas with respect to population size, economic activities and population density (Van Duijne & Nijman, 2019). Urbanizing areas emerging in rural-urban transition regions are normally small and cross administrative boundaries of towns and villages (Van Duijne & Nijman, 2019). Therefore, they cannot be found by population census data and are typically neglected by the government, hindering the understanding of the actual urbanization process in small regions.

Remote sensing imagery from the earth surface contains detailed land cover information and can contribute to urban area mapping and urban dynamic analysis such as the conversion from rural into urban areas (Yang, Xian, Klaver, & Deal, 2003). Approaches based on remote sensing data, often in combination with spatial metrics (Reis, Silva, & Pinho, 2016), can help researchers to position where changes are happening, and analyse how human activities affect urban development (Mubako et al., 2018). Based on this spatial information of urbanization processes, researchers and urban planners can evaluate existing urban development strategies and further plan accordingly. TerraSAR-X imagery was used to map the Global Urban Footprint to support urban dynamics analysis in the world (Esch et al., 2018). Besides, spatial analysis based on satellite images is widely implemented by many governments and academic institutions at local, national and global levels to monitor urban growth and analyse urban dynamics (Ji et al., 2001). For example, the GHS Urban Centre Database(GHS-UCD) (2019) extracted built-up areas from satellite images and combined them with population data to delineate urban centres at the global level. But the coarse resolution does not cover small urbanizing regions well. A study that aimed at high spatial detail was the e-Geopolis programme (e-Geopolis Institute, n.d.), however, they delineated contiguous built-up areas manually, which is time-consuming and labour-intensive.

Computational methods applied to VHR satellite images can help to extract detailed land cover/use information and can help to analyse patterns of urban settlements. However, it is still difficult to accurately classify land cover/use from VHR images because of the complex structure of urban areas and the big data volume (Mboga et al., 2019). Now deep learning algorithms like FCN can extract spatial features in satellite images by learning the neighbourhood information of pixels and therefore has the ability to classify complex land cover/use types (Wu et al., 2019).

Thus, this study will focus on generating an FCN-based approach to delineate urbanizing areas of small regions and analyse the dynamics of urbanizing areas in a semi-automatic way. The research objectives will be further introduced in section 1.3.

1.2. Research problem identification

There are different definitions of urban nowadays and they will be further introduced in section 2.1. Most of them relate to the contiguity of built-up areas and population size. The government of India ignores some small urbanizing areas because they are not visible in the census data collected according to the administrative units (Denis & Marius-Gnanou, 2010). For example, some officially defined towns and villages possibly form a contiguous built-up agglomeration which can be considered as in situ urbanizing areas, but these newly formed agglomerations are not registered as urban by the government; this phenomenon has happened in India, and some countries in the Global South such as Tanzania and Ethiopia are likely to have the same situation(Van Duijne & Nijman, 2019). However, there is no detailed spatial information on these urbanizing areas which are mainly located in rural-urban transition zones.

Furthermore, regarding the datasets used for delineating urbanizing areas, neither the governmental data (e.g. census data) nor the frequently used disaggregated census data products like the population grid data from WorldPop (2018) provide information that would allow delineating urbanizing areas in small regions. Besides, although some efforts have been made to manually delineate contiguous built-up areas through visual interpretation of satellite images (Denis & Marius-Gnanou, 2010), these are not efficient ways and do not allow for frequent updates. In order to respond to this shortcoming, this thesis makes use of advanced techniques for land cover/use classification to automatically delineate and spatially characterize urbanizing areas using machine learning and spatial analysis.

1.3. Research objective

1.3.1. General objective

The research objective in this study is to develop an FCN-based approach to analyse the spatial dynamics of urbanizing areas of small regions in a semi-automatic manner.

1.3.2. Specific objectives

1. To classify land cover/use classes from satellite images using FCN.
2. To delineate urbanizing areas of the study area at different time points.
3. To analyse the spatial dynamics of urbanizing areas in the study area over time.

1.4. Research questions

1. To classify land cover/use from satellite images using FCN.
    - What is a meaningful distinction of land cover/use classes to describe the dynamics of urbanizing areas?
    - What is a suitable data pre-processing strategy for training and testing the FCN?

  - What is the accuracy of land cover/use classification result?
2. To delineate urbanizing areas of the study area at different time points.
  - What is a suitable method to delineate contiguous built-up areas at different time points?
  - What is a suitable method to disaggregate census data to contiguous built-up areas at different time points and identify urbanizing areas?
3. To analyse the spatial dynamics of urbanizing areas in the study area over time.
  - What are the changes of spatial patterns of contiguous built-up areas?
  - How does the population change in urbanizing areas over time?
  - What kind of urbanization trend is visible in this study area?

1.5. Thesis structure

This thesis contains five chapters:

- Chapter 2 reviews literatures related to the urban definition, methods used for land cover/use classification and census data disaggregation, and the analysis for urban patterns and urban development processes.
- Chapter 3 introduces the study area and elaborates the methods adopted in this study, including methods used for land cover/use classification, urbanizing areas delineation, and indicators used for analysing urban dynamics of the study area. Datasets used in this study are also introduced in this chapter.
- Chapter 4 presents and discusses the results achieved in this study.
- Chapter 5 summarizes findings of this study and makes recommendations for further research.

2. LITERATURE REVIEW

In this chapter, the first section introduces different definitions of urban. The second section provides an overview of researches regarding land cover/use classification based on remote sensing data and introduces the principles of artificial neural networks. The next section presents different approaches for census data disaggregation and the final section introduces different types of urban growth trends and different spatial metrics used for analysing the urban dynamic.

2.1. Definition of urban

The definition of urban affects the quantification of the degree of urbanization in a region. Since the 1950s, there have been discussions on the definition of urban (Brenner & Schmid, 2014). Kingsley Davis, a scholar who engaged in the earliest debates on this topic, defined cities as regions with more than 100,000 people based on empirical research (Brenner & Schmid, 2014). However, Louis Wirth argued that the definition of a city based solely on population is too rough and may be misleading, because the population essentially spans across administrative boundaries (Wirth, 1938). Nowadays, there are still no standardized definitions on urban at the global scale. Some countries define urban only according to different population sizes within administrative units; some countries based their definitions on more comprehensive criteria referring to economic activity, population size and the extent of built-up areas (United Nations, 2017). The United Nations publishes urban demography data based only on the urban population provided by countries according to their own national definitions.
However, there are still many scholars trying to propose unified definitions of urban in order to conduct comparative research on urbanization in the world. For instance, Denis and Marius-Gnanou (2010) put forward a general definition for urban in the context of the e-Geopolis project: an agglomerate with more than 10,000 people and consecutive built-up areas where the gap between built-up areas is less than 200 metres. Another global definition of urban is put forward by the European Commission (2019); it defines urban centres as areas that consist of continuous grids which are more than 1 square kilometre, with more than 50,000 people and the population density is more than 1,500 persons per square kilometre. However, the size of continuous grids in this definition maybe not suitable for some relatively small-scale cities and towns which are only a few square kilometres large. Both approaches show that the definition of the urban area according to the land cover and demographic information deviates from the bondage of administrative boundaries and support the analysis of the actual urban growth and urbanization patterns (Denis & Marius-Gnanou, 2010).

2.2. Land cover/use classification

2.2.1. Overview of methods for land cover/use classification

Land cover/use classification means classifying land cover/use classes from remote sensing images. Different parametric and non-parametric methods have been applied to do land cover/use classification to derive spatial information of urban and rural areas. An example of a parametric supervised classifier is Maximum likelihood Classification (MLC) which requires normally distributed classes. MLC is widely applied by researchers, such as Stefanov, Ramsey and Christensen (2001), who adopted this method on Landsat Thematic Mapper data to classify eight land cover classes in Phoenix, USA. Non-parametric methods include decision trees (McIver & Friedl, 2002), support vector machine (SVM) (Pal, 2008), random forest (Gislason, Benediktsson, & Sveinsson, 2006), artificial neural networks (ANN) (Volpi & Tuia, 2017) and so on.

Some studies also compared the performance of these methods on doing land cover/use classification. For instance, Srivastava et al. (2012) found that ANN performed better than SVM and MLC in terms of classification accuracy after testing these methods on the same datasets, but ANN required longer running time. And other researches (Liu, Abd-Elrahman, Morton, & Wilhelm, 2018; Yoo, Han, Im, & Bechtel, 2019) also proved that using ANN such as FCN and Convolutional neural networks (CNN) to do land cover/use classification is gaining popularity in recent years and the classification accuracy is higher than other methods. This study regards obtaining classified maps with high accuracy as the priority, rather than the time and computational cost, because the study area is relatively small, and the identification and dynamic analysis of urbanizing areas requires precisely classified built-up areas. Therefore, this study applied FCN to do the land cover/use classification.

2.2.2. Deep learning algorithms

As elaborated above, deep learning algorithms such as CNN and FCN are adopted in many studies to derive classified land cover/use maps, which can be further used to delineate urbanizing areas. Classifying land cover/use types from VHR images is difficult, especially in urban areas, since some land cover/use classes are with complex texture and influenced by some factors such as illumination; however, the deep neural network can automatically learn the deep-level features of classes, so as to carry out accurate classification (Fu, Liu, Zhou, Sun, & Zhang, 2017).

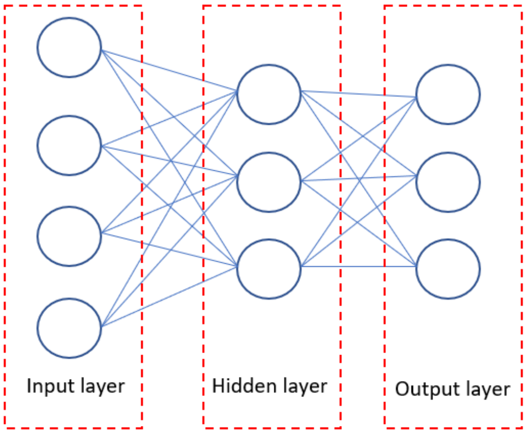

Figure 1. An example of ANN architecture

Generally, FCN and CNN are categories of ANN, which structure looks similar to biological neural network (Chen, Lin, Kung, Chung, & Yen, 2019). An ANN consists of three kinds of layers, which are the input layer, the hidden layers, and the output layer. One example of an ANN architecture is shown in Figure 1. The input layer consists of images to be classified. And operations take place at the hidden layers and output layers allow to extract characteristics from images and produce outputs. The number of hidden layers is not constrained and decided by the designer. In two adjacent layers, all neurons (blue circles in Figure 1) are connected to each other. The activated value z of a target neuron in ANN is calculated based on Equation 1 (Nielsen, 2015), where σ is the activation function and x_i is the neuron i in the previous layer, and w_i is the weight of neuron i and b_i is the bias of the target neuron.

$$z = \sigma(\sum_i w_i x_i + b_i) \quad \text{(Equation 1)}$$

The activation function σ is used to determine whether a neuron needs to be activated for further learning. Hidden layers in CNN are convolution layers followed by fully connected layers. Convolutional operations are done in convolution layers and the image size is reduced by down-sampling to extract more characteristics from the image. An example of the convolution operation is presented in Figure 2. Fully connected layers are at the end of the network, taking results from previous layers and producing the final class of the input image (Bergado, Persello, & Gevaert, 2016).

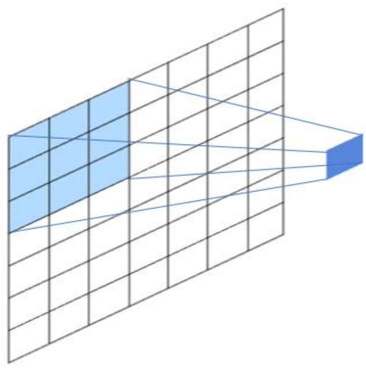
Figure 2. An example of the convolution operation (Source: Author)

CNNs can be used for image classification and the output is a single label for each image. Therefore, if image classification at the pixel level (named as semantic segmentation) is required, training CNN will lead to redundant image processing procedures and the computational cost will be high when dealing with large images (Persello & Stein, 2017). FCN can be used for semantic segmentation, because FCN have the same architecture as CNN except for the last few convolution layers, which can classify the image pixel by pixel (Zhang et al., 2018). One common way to derive labels for each pixel is up-sampling after down-sampling by deconvolution in networks. As suggested by Nielsen (2015), the number of convolution layers needs to be carefully structured when training FCN, because deeper networks can extract more features, but more location information can be lost, making the output rougher. The architecture used in this study is introduced in section 3.4.3.

2.3. Census data disaggregation

Urbanisation studies typically rely on population statistics, collected either through a census (e.g. India, China) or by means of registration (e.g. the Netherlands). The census is the process of collecting and organizing population data and related social and economic data of a country or a designated area within a certain period, which can be used as basic datasets for policy making, academic research and other purposes (United Nations, 2008).

Commonly, census data are made available for large and aggregated spatial units. In order to obtain spatially distributed population information, various methods are used for disaggregating census data. The Gridded Population of the World (GPW) provides population grids obtained by distributing census data evenly over grids that cover each region (Balk et al., 2006). In addition, the Global Rural Urban Mapping Project (GRUMP) allocated population based on the methods used by GPW, but GRUMP found the location of urban areas using nightlight information first and allocated the rural population and urban population separately (Da Costa, Calka, & Bielecka, 2017). Stevens et al. (2015) developed a random forest model based on various datasets including the location of roads and other land cover information to estimate the gridded population density and subsequently derived the population grids by combining census data. Moreover, Freire, Aubrecht and Wegscheider (2011) applied an 'intelligent dasymetric mapping' approach by disaggregating census data based on land cover/use data and the distribution of workers and students at daytime. In their research, the population distribution at day and night was estimated respectively to analyse the human exposure to tsunami in Lisbon, Portugal. Grippa et al. (2019) also applied dasymetric mapping to reallocate population census data collected at the administrative level to 100 metre by 100 metre grids. They estimated the population density of each grid based on land cover/use maps created from satellite images and reallocated the population accordingly to obtain the population distribution at sub-administrative level. These cases indicate that a variety of data sources, especially remote sensing data such as satellite images, including night-time light data, can be used to provide land cover/use information and information related to human activity to support the population disaggregation, making the population estimation on a smaller scale more realistic. Methods and assumptions used in this study are introduced in section 3.5.2.

2.4. Analysis of urban patterns and urban growth trends

2.4.1. Spatial metrics and urban pattern analysis

Several studies have used spatial metrics to quantitatively characterise urban patterns and support urban pattern comparison between different regions and the analysis of urban pattern changes over time. Generally, spatial metrics are measurements calculated based on thematic maps, representing the spatial heterogeneity of the landscape (Martin, Couclelis, & Clarke, 2005). They are commonly calculated at the patch level (Gustafson, 1998). Patches are defined as homogenous areas symbolizing the landscape category of interest, such as 'non-built-up area' and 'road' (Martin et al., 2005). In addition to analysing the spatial characteristics of landscapes, spatial indicators can also be used to analyse the dynamic changes in

landscape categories of interest when applied to geographic data on multiple periods (Dunn, Sharpe, Guntenspergen, Stearns, & Yang, 1991).
Studies have employed different spatial metrics to quantify spatial characteristics of the urban area and did comparison of urban patterns among cities. For instance, to analyse urban patterns of twelve cities in India, Taubenböck et al. (2009) calculated the urban area and built-up density to have an initial analysis of the degree of urbanization in these cities; the compactness and shapes of urban areas in these cities were analysed by calculating largest patch index (LPI), patch density (PD), landscape shape index (LSI), number of patches (NP), edge density (ED) and total edge (TE). Seto and Fragkias (2005) analysed the spatial patterns of four cities in China using multiple spatial metrics from three aspects: the absolute size of urban areas (evaluated by the areal extent of urban areas and NP), the relative size of urban areas (analysed based on the mean patch size) and the complexity of urban areas (analysed based on area-weighted mean patch fractal dimension and ED).

2.4.2. Analysis of urban growth trends

In general, there are three types of urban growth trends: infill (Figure 3(a)), expansion (Figure 3(b)) and outlying (Figure 3(c)) (Dutta & Das, 2019). The infill type of urban growth means that the newly emerged urban area is located mostly within the original urban area, replacing the original urban vacant land (Ellman, 1997). While in the case of expansion, the urban growth happens when the newly emerged urban areas are mainly located at the fringe of the existing urban area, thereby enlarging the urban area by growing outwards (Wilson, Hurd, Civco, Prisloe, & Arnold, 2003). And the outlying urban growth means that the new urban area is spatially isolated from the original urban area (Dutta & Das, 2019).

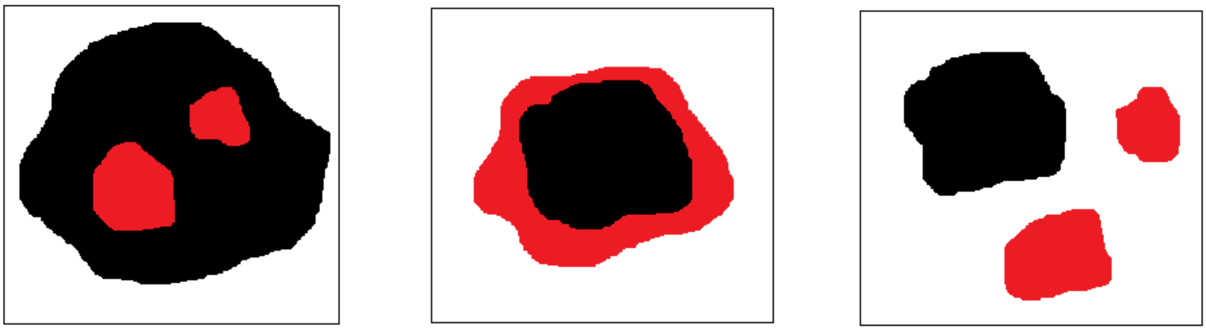

(a) (b) (c)

Figure 3. Three types of urban growth (Black polygons are old urban areas and red polygons are newly emergent urban areas. (a): infill; (b): expansion; (c): outlying; Source: Author)

Studies have applied various spatial metrics to analyse the urban growth trend over time. For instance, by calculating and interpreting spatial metrics including LSI, Nearest-Neighbour distance, Aggregation Index and ratio of open space, a study on the English Bazar, India found that urban expansion mainly occurred in suburban areas from 1991 to 2016, while new urban areas emerged far away from the core city (outlying growth) after 2001 (Dutta & Das, 2019). Moreover, Terfa et al. (2019) used NP, Class Area and Percentage of Landscape as spatial metrics to analyse urban growth of three big cities in Ethiopia and two of them (Addis Ababa and Adama) showed decentralized urban sprawl, while Hawassa experienced compacted urban growth conversely.
To summarize, spatial metrics used for urban pattern analysis and urban growth trend analysis in the above studies were mainly selected from three aspects: the areal extent and the complexity of urban areas, and the degree of aggregation of urban areas, to show spatial characteristics of the study area. They also try to avoid choosing spatial metrics with strong correlation. The choice of spatial metrics used in this study is introduced in section 3.6.

3. METHODOLOGY

3.1. Study area

The study area is the Barharia cluster, located in the Indian state Bihar, and consisting of six settlements. According to the census data in 2001, India showed considerable urban growth probability due to the high natural growth rate and prosperous economic development, but in reality, at that time, the urbanization rate of India was still very low (Denis & Marius-Gnanou, 2010). This phenomenon shows that the degree of urbanization in India may be underestimated, and the changes happening at the rural-urban transition zone may be ignored by census data (Van Duijne & Nijman, 2019).

The choice of the study area relates to a PhD project ("A New Urban Epoch? Alternative ways to measure urbanization using VHR remote sensing data," n.d.) focusing on urban formations of India. This master thesis will provide more detailed information on the urban dynamics of the Barharia cluster and contribute to this research. In the study area, none of the settlements is defined as urban in the Census of India. However, according to the Census in 2001 and 2011, the population size and population density increased significantly in these settlements, and the percentage of people engaging in non-farm works in these settlements increased by 40% on average from 2001 to 2011. Survey data on 162 companies collected in the above-mentioned PhD project in the Barharia cluster in 2018 indicates that about 74% of these companies have been established within 10 years. About 60% of companies belong to the retail industry and some service companies also exist in this region. Interview data on people's daily lives in that region (also collected by the PhD fieldwork) shows that residents in the past needed to go to Siwan, which is the nearest city to the Barharia cluster, to buy all the daily necessities. But now they can buy the necessary items locally, and only need to go to Siwan when they need health care. Therefore, from the social and economic profile of this region, we could imagine that this region is gradually developing into a city.

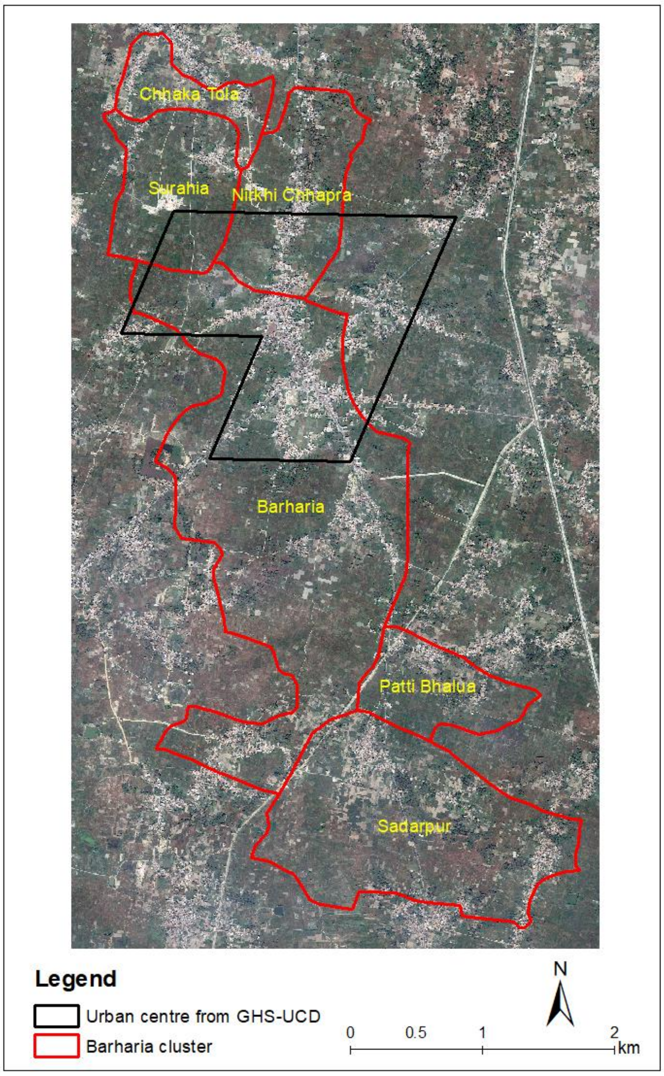

Figure 4. The Barharia cluster. (Data source: the GHS Urban Centre Database (2019), shapefile from PhD candidate van Duijne, R. J., the University of Amsterdam; WorldView-2 image in 2018)

Moreover, as can be seen from the satellite image (shown in Figure 4), there are contiguous built-up areas across these settlements, suggesting that the area is urbanising. Over plotting the boundaries of the urban centre data product, we can also notice that the urban areas delineated by the GHS-UCD (2019) are not accurate in small regions such as this study area. Therefore, there is a big chance that the Barharia cluster contains urbanizing areas which are neglected by the Census and global datasets such as the GHS datasets.

3.2. General approach

In order to delineate urbanizing areas across administrative boundaries, this study adopted the definition used by Denis and Marius-Gnanou (2010), and analysed the dynamics of these areas based on the delineation. This study employed five steps, namely 1) satellite image classification, 2) delineation of contiguous built-up areas, 3) modelling population for contiguous built-up areas, 4) identification of urbanizing areas, 5) analysing the urban dynamics. Analysing an urbanizing area over a long period (here 13 years) can help revealing the urban development process in the study area. The analysis considered and compared urbanizing areas of 2005, 2010 and 2018, because the satellite images with a spatial resolution of sub-meter level could be obtained for those years.

The flowchart of this study is shown in Figure 5 and the main procedures in each step are briefly explained here. First, classified maps of 2005, 2010 and 2018 were obtained from satellite images by doing land cover/use classification using FCN. Three classes were classified in this study: built-up areas, roads and non-built-up areas. This study is most interested in the built-up area, while roads are expected to be separated from the built-up area, which mainly contains residential and commercial activities. Classifying built-up areas for the three time stamps can show the growth trajectory of the built-up area. In contrast, non-built-up areas include bare soil lands, forests, agricultural lands and water body. Built-up areas were extracted from the classified maps and were aggregated to delineate contiguous built-up areas. Then, contiguous built-up areas, local census data and the shapefile of settlements in the Barharia cluster were used to estimate the population of each contiguous built-up area at different years. Urbanizing areas were derived by selecting contiguous built-up areas with more than 10,000 residents. Finally, information derived by calculating indicators of three aspects (the urban areal extent change, morphological changes of built-up areas and population changes) as well as land consumption efficiency were used to analyse the dynamics of urbanizing areas. Besides, we also analysed the improvement of the living environment of the study area from a qualitatively perspective by comparing the quality of houses and roads of one example area from VHR images in 2005, 2010 and 2018.

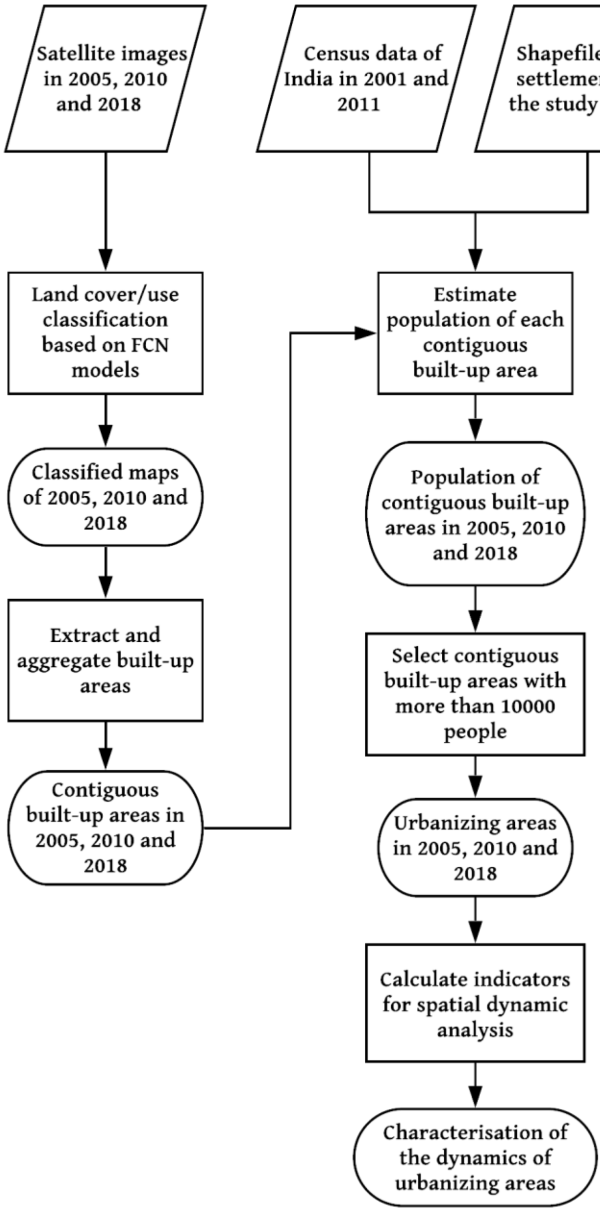

Figure 5. The flowchart of this study

3.3. Data description

The datasets employed in this study consist of VHR satellite images for 2005 (QuickBird-2 satellite), 2010 and 2018 (WorldView-2 satellite, respectively) for the land use classification, as well as the shapefile of the Barharia cluster and the census data of 2001 and 2011 to estimate the population of the Barharia cluster (Table 1). The WorldView-1 satellite and the WorldView-2 satellite was launched in 2007 and 2009 respectively. Therefore, we had to choose images captured by the QuickBird-2 satellite (launched in 2001) for having a longer time span. We wrote a detailed data request proposal which described the background, objective, methods, and anticipated results of this study to the European Space Agency (ESA). The requested VHR satellite images were obtained for free after the approval of ESA. The VHR satellite images were pre-processed according to the description in section 3.4.1.

Table 1. Summary of the dataset

Data	Time	Description
QuickBird-2 satellite image	June, 2005	4 bands; Resolution: Panchromatic band: 0.6 m×0.6 m Multispectral bands: 2.4 m×2.4 m
WorldView-2 satellite image	March, 2010	8 bands; Resolution: Panchromatic band: 0.5 m×0.5 m Multispectral bands: 2 m×2m
WorldView-2 satellite image	March, 2018	8 bands; Resolution: Panchromatic band: 0.5 m×0.5 m Multispectral bands: 2 m×2m
Shapefile of the Barharia cluster	2018	Administrative boundaries of settlements within the Barharia cluster, provided by PhD candidate Van Duijne, R. J., from the University of Amsterdam
Indian census data	2001	Population of the Bihar state in 2001
Indian census data	2011	Population of the Bihar state in 2011

3.4. Land cover/use classification

3.4.1. Pre-processing of the data

Prior to the land cover/use classification, the satellite images of each year were pan-sharpened using the Hyper-spherical Colour Sharpening algorithm, which is designed for the WorldView-2 data. Therefore, all the multispectral bands of the satellite images have the same resolution as the panchromatic bands.

Another pre-processing step is the generation of tiles since the land cover/use classification requires tiles that cover small parts of the total study area, as explained in a study related to informal settlements detection (Persello & Stein, 2017). Tiles used for training FCNs need to contain enough training samples of each class. However, most areas on satellite images of the Barharia cluster are non-built-up areas. Therefore, tiles used for training and testing FCNs are selected based on the following rules:

1) Selected tiles need to cover all three classes and the size of each tile is not larger than 2000×2000 pixels.

2) Selected tiles need to cover built-up areas of the study area as much as possible to provide sufficient training samples for the classification of built-up areas, because this is the class that we are most concerned in this study.

3) All tiles from images in 2010 and 2018 and most tiles from the image in 2005 need to be located within the Barharia cluster. Some tiles from the image in 2005 are allowed to be located in the surroundings of the Barharia cluster to guarantee enough training samples for the 'built-up area' class, because the built-up area within the study area in 2005 is considerably smaller than in the other two years.

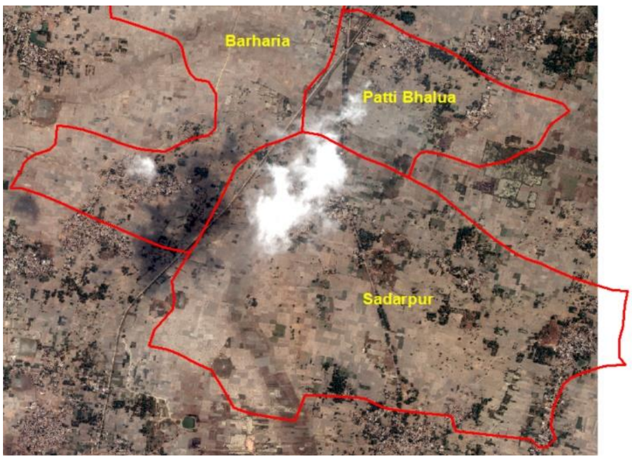

Figure 6. The area covered by clouds in the satellite image of 2005 (Data source: QuickBird-2 satellite image in 2005; shapefile of the study area from PhD candidate van Duijne, R. J., the University of Amsterdam)

Based on these rules, thirteen tiles were selected with a size of 2000×2000 pixels from the image in 2018 and 2010. As for the satellite image of 2005, eleven tiles with the size of 2000×2000 pixels were selected within or in the surroundings of the study area. These tiles cover the majority of the study area except for the south-western part, which is covered by some clouds on the image (shown in Figure 6).

3.4.2. Reference data preparation

Reference maps were obtained by visual interpretation of each tile in each year. Classes and their corresponding labels are shown in Table 2. The visual interpretation was made by drawing polygons with labels that cover corresponding classes on each tile. Figure 7 shows an example of the visual interpretation for one tile in 2018. The reference map for each tile was obtained by converting corresponding polygons to the file in TIFF format. Pixels that are not labelled were assigned the value 0 and were not trained in the network.

Table 2. Land cover/use classes and labels in the reference map

Class	Label
Built-up area	1
Road	2
Non-built-up area	3

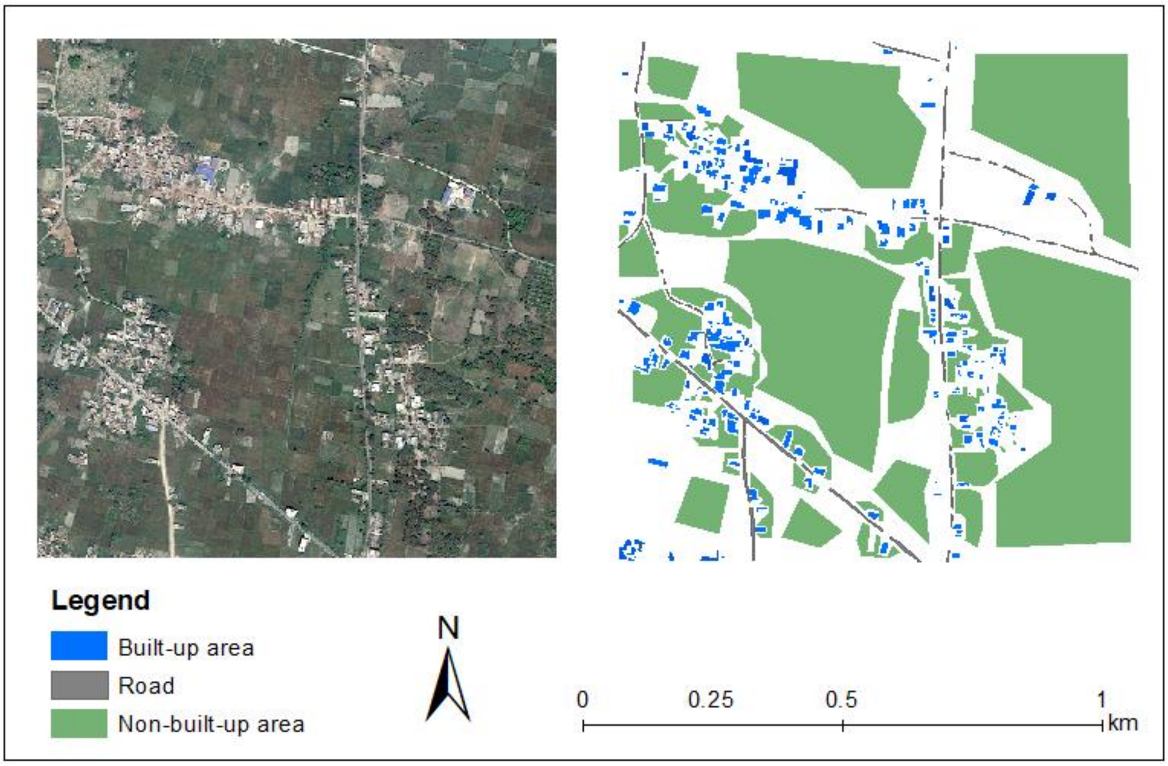

Figure 7. The visual interpretation for one tile in 2018 (image on the left: a training tile of 2018, Data source: WorldView-2 image in 2018; figure on the right: the corresponding reference map)

3.4.3. FCN architecture

This study adopts the FCN architecture with dilated kernel (FCN-DK), which performed well on land cover/use classification related to informal settlements, developed by Persello and Stein (2017). Therefore, it also has the possibility to precisely classify land cover/use classes in this study. This FCN architecture is shown in Table 3. The major part of the network is convolutions with different number of filters. The kernel size is 5×5 for the first six blocks and 1×1 for the output block. Stride indicates the interval between the centre of convolution kernels (stride=1 means interval of one pixel). The padding parameter defines the number of zeros added to the border of the image. In FCN-DK, this is defined for keeping the size of the output image the same as the input image after each convolution. The dilation factor means the intervals adding between the cells in filters (dilation=1 means interval of one pixel). Convolutions with a dilation factor can increase the receptive field - meaning the learning area of a neuron in neural networks - without adding additional parameters (Yu & Koltun, 2016). Figure 8 shows an example using a 3×3 filter, demonstrating the change of receptive fields with different dilation factors. The red dots in Figure 8 represent cells of the filter, and the blue cells represent the receptive fields that can be perceived during the training.

The activations used between convolutions are Leaky rectified linear units (leakyReLU) (Wang et al., 2018). LeakyReLU can avoid the problem that with the increase of convolution layers, the gradient decreases, which in turn causes the neural network to converge slowly. The output block consists of a 1×1 convolution layer and a softmax function to convert the multi-classification results into non-negative numbers and map them between 0 and 1, and finally produce the probability that the pixel belongs to a certain class.

Table 3. The FCN architecture used in this study

Block	Layer	Dimension	Stride	Pad	Dilation
FCN-DK1	Convolution leakyReLU	5×5×8×16	1	2	1
FCN-DK2	Convolution leakyReLU	5×5×16×32	1	4	2
FCN-DK3	Convolution leakyReLU	5×5×32×32	1	6	3
FCN-DK4	Convolution leakyReLU	5×5×32×32	1	8	4
FCN-DK5	Convolution leakyReLU	5×5×32×32	1	10	5
FCN-DK6	Convolution leakyReLU	5×5×32×32	1	12	6
Output	Convolution Softmax	1×1×32×3	1	0	1

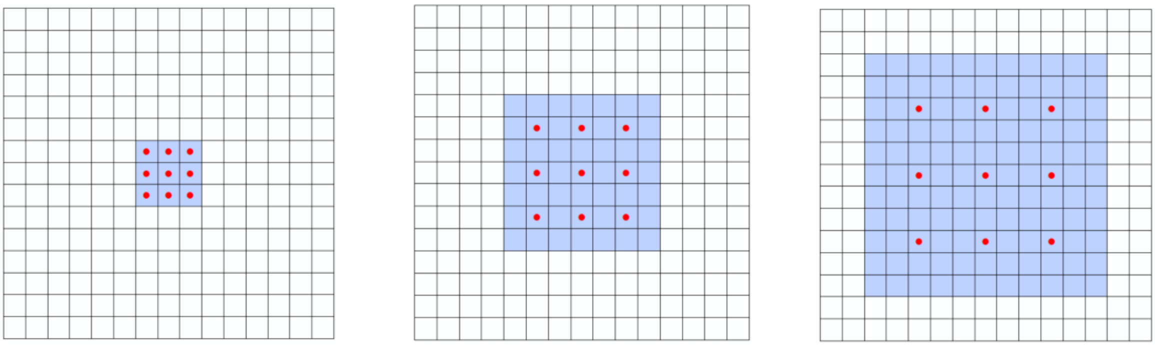

(a) (b) (c)

Figure 8. The example of receptive field of the dilated kernel ((a): dilation = 1, receptive field = 3×3; (b): dilation = 2, receptive field = 7×7; (c): dilation = 3, receptive field = 11×11)

3.4.4. Training networks

For each year, the FCNs were trained using stochastic gradient descend algorithm (momentum = 0.9). The networks were implemented in Python using TensorFlow. There are somewhat more training tiles than testing tiles to ensure enough training samples are used as input to help the network to extract characteristics of classes. The selection of training and testing tiles is done randomly. As for the image in 2010 and 2018, eight and five tiles were used for training and testing respectively. For the image in 2005, seven tiles were used for training and four tiles were used for testing. The networks were trained initially with the learning rate of 0.0001 and 100 epoch (Liu, Kuffer, & Persello, 2019) and the parameters were adjusted according to the loss and accuracy in each training.

3.4.5. Accuracy assessment

The accuracy of the FCN networks was assessed by three indices calculated based on the confusion matrix (Foody, 2002), specifically precision, recall and F1score (Equation 1-3). They can help evaluate the accuracy and reliability of the FCN model. For each class, its precision is defined as the ratio of the number of pixels that are correctly classified in the prediction map to the number of pixels that are all classified into this class (calculated using Equation 1). The recall of each class is defined as the ratio of the number of pixels that are correctly classified in the prediction map to the number of pixels that belong to this class in the reference map (calculated using Equation 2). F1-score is calculated based on the precision and recall of the FCN model (shown in Equation 3), helping evaluate the performance of the model comprehensively. In the confusion matrix, for class i, n_{ii} represents the number of truly classified pixels of class i; $n_{i\sim}$ means the total number of pixels in the row; $n_{\sim i}$ means the total number of pixels in the column. The equations of precision, recall and F1-score are shown as follows:

$$precision = \frac{n_{ii}}{n_{\sim i}}$$ *Equation 1*

$$recall = \frac{n_{ii}}{n_{i\sim}}$$ *Equation 2*

$$F1\_score = \frac{2 \cdot precision \cdot recall}{precision + recall}$$ *Equation 3*

3.5. Urbanizing area delineation

3.5.1. Generate contiguous built-up areas

Following the definition of urbanizing areas introduced by Denis and Marius-Gnanou (2010) (see also in section 2.1), we regard built-up areas with a mutual distance of less than 200 metres as continuous built-up areas. For each year, all classes are extracted from classified maps and saved as polygons respectively. Two rules were followed in this study to remove some noises between and within classifications:

(1) The minimum size of built-up areas is 15 square meters. Since the standard of the minimum size of houses varies and depends on local circumstances, the minimum size was determined by empirical explorations of the size of houses in the satellite image. In the study area, the common size of a small single house area is about 15 square metres.

(2) Following Pesaresi et al. (2016), we assume that only unidirectional expansion of built-up areas is assumed to take place over time in the study area, which means that the built-up areas will be removed if they existed in early years but not in the most recent year. This consistency rule together with the former rule can remove some areas that were misclassified into built-up areas by FCN, eliminating some interference with the subsequent delineation of contiguous built-up areas.

Therefore, first, the polygons representing built-up areas in 2018 were clipped by the boundary of settlements in the Barharia cluster, and polygons that are smaller than 15 square meters were removed. And then, similarly, the built-up areas in 2010 and 2005 were derived one by one using the same methods, based on the rules we introduced before.

Polygons representing built-up areas were aggregated to form contiguous built-up areas using the 'aggregate polygons' tool in ArcGIS. This tool can aggregate polygons when the boundaries of these polygons are within a certain distance. An example is shown in Figure 9: the purple polygons are aggregated together to form a new blue polygon. In this study, polygons were aggregated when the distance between them is less than 200 metres.

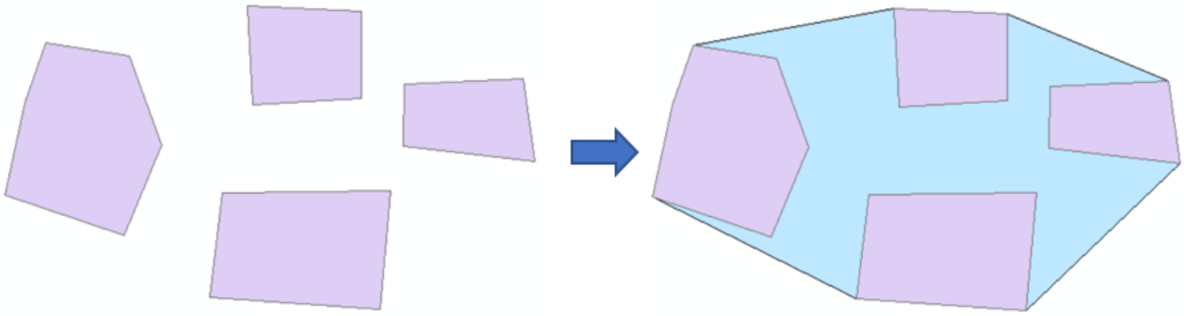

Figure 9. An example of the application of 'aggregate polygons' tool in ArcGIS (Source: Author)

3.5.2. Population estimation

Census data for 2001 and 2011 in India were used as the source to estimate the population of each settlement in 2005, 2010 and 2018 respectively. This study assumes that the population growth rate between 2001 and 2011 is maintained from 2011 to 2018. This study also assumed that the population growth rate of the state Bihar is more appropriate for the circumstances of the Barharia cluster than the annual growth rate of the entire country (1.55%, according to the World Bank (2018)). Following the World Bank approach, the average growth rate of the state Bihar was determined according to Equation 4 using the census data of 2001 and 2011, where r represents the average population growth rate in t years; N_t means the population of the last year and P_0 means the population of the first year. Applying equation 4, we got a result of 2.3% in Bihar, which is higher than the whole country.

$$r = \frac{\ln\left(\frac{N_t}{P_0}\right)}{t} \qquad \textit{Equation 4}$$

Subsequently, for each year of this study (2005, 2010 and 2018), the population of each settlement was calculated using the census data and the population growth rate derived from Equation 4.

The population of each contiguous built-up area was estimated using the following assumptions and methods. This study assumes that the population is evenly distributed over contiguous built-up areas. However, the contiguous built-up areas often cross the administrative boundaries of settlements. Therefore, the population for each built-up area cannot be directly computed. As we already got the population of each settlement, contiguous built-up areas that cross the boundaries of settlements were split into pieces according to the administrative boundaries of settlements in the study area first, and then, these pieces were again merged into contiguous built-up areas after re-calculating the population assigned to these pieces, based on their share of area. Therefore, the population assigned to each contiguous built-up area in each settlement is estimated according to the proportion of the area of each contiguous built-up area to the total area of the contiguous built-up area within each settlement (Equation 5). In this equation, i represents the settlements and j represents the contiguous built-up area in the settlement.

$$population\ of\ builtup\ area_{ij} = population_i \times \frac{the\ area\ of\ the\ contiguous\ builtup\ area_{ij}}{total\ contiguous\ builtup\ area_i} \qquad \textit{Equation 5}$$

3.5.3. Urbanizing areas delineation

After obtaining the contiguous built-up areas and population of each contiguous built-up area, areas with more than 10,000 people were identified as urbanizing areas. However, urbanizing areas were only computed for those areas for which we had cloud-free image data. Therefore, in 2005, the urbanizing areas within Sadarpur settlement could not be delineated. Besides, the area covered by clouds in Patti Bhalua settlement is not affected when doing the urbanizing area delineation, because almost no buildings were in this area after checking the VHR image visually.

3.6. Indicators of urban dynamics analysis

As we mentioned in section 2.4, studies normally analysed the dynamics of urban areas from the areal extent, complexity, and the degree of aggregation aspect. Spatial metrics should be selected according to the specific research objective and study area (Parker, Evans, & Meretsky, 2001). In this study, we concentrate on delineating and characterising urbanizing areas and analysing how the urbanizing area formed and developed. Therefore, spatial metrics characterising the degree of aggregation of contiguous built-up areas were selected to capture the morphological changes of the contiguous built-up area in the study area.

Additionally, the analysis of the dynamics of urbanizing areas also includes changes in the urban areal extent of the study area and changes of population in urbanizing areas. The areal extent of urbanizing areas at different years was calculated to estimate urban expansion of the study area within the studied period (2005-2018). Besides, population size, population density of urbanizing areas and the proportion of population in urbanizing areas compared with the whole cluster were calculated to show population changes of urbanizing areas. The summary of indicators is shown in Table 4. By interpreting the outcomes of these three aspects, the dynamics of urbanizing areas in the study area can be analysed.

Table 4. The summary of indicators used in the analysis of the dynamics of urbanising area

Factors	Indicators	Explanation
Urbanizing areal extent change	The areal extent of urbanizing areas (ha)	This indicator aims to show whether urbanizing areas increase or not (Taubenböck et al., 2009).
Morphological change of contiguous built-up areas	Built-up density $= \frac{\sum_{i=1}^{m} a_{ij}}{a_t} \times 100\%$	a_{ij} is the area (m²) of contiguous built-up area i in year j and a_t is the total area (m²) of the study area. This indicator shows the degree of the contiguous built-up area occupying the area of administrative units (Taubenböck et al., 2009).
	Number of patches (NP)	The number of patches representing contiguous built-up areas in the Barharia cluster in each year. The more patches, the sparser of the built-up area (Ramachandra, Aithal, & Sanna, 2012).
	Largest patch index (LPI) $= \frac{\max(a_{ij})}{a_t} \times 100\%$	$\max(a_{ij})$ is the area (m²) of the largest contiguous built-up area in year j and a_t is the total area (m²) of the study area. It shows whether the largest patch is more dominant over time (Taubenböck, Wurm, Geiß, Dech, & Siedentop, 2019).
	Mean Euclidean nearest neighbour distance (ENN_MN)	d_{ij} is the shortest distance (m) between contiguous built-up area i and its neighbour contiguous built-up area in year j and n_j is the number of distance

	$= \frac{\sum d_{ij}}{n_j}$	calculated in year j. It indicates the degree of density of the contiguous built-up area (Dutta & Das, 2019).
	Aggregation index (AI) $= \frac{e_i}{\max(e_i)} \times 100\%$	e_i is the number of adjacent edges of the cells in the contiguous built-up area and $\max(e_i)$ is the maximum adjacent edges that these cells can have, showing the compactness of the contiguous built-up area (Ramachandra et al., 2012).
Population change	Population density of urbanizing areas $= \frac{p_i}{a_i} \times 100\%$	p_i is the population of the urbanizing area in year i and a_i is the area of the urbanizing area in year i (Bertaud, 2001).
	The total population of urbanizing areas	This indicator shows whether the population living in the urbanizing area increased or not over time (Bertaud, 2001).
	The proportion of population in urbanizing areas compared to the whole cluster $= \frac{p_i}{p_{ti}} \times 100\%$	p_i is the population of the urbanizing area in year i and p_{ti} is the total population of the Barharia cluster in year i. This indicator shows the degree of population covered by the urbanizing area (Zhou & Ma, 2005).

As for the calculation of spatial metrics, the contiguous built-up areas of the Barharia cluster in each year were converted to raster first, and the raster was used to calculate these spatial metrics. Spatial metrics are calculated and standardized to a value between 0 and 1 using Equation 6 (Rowley, Peters, Lundie, & Moore, 2012), facilitating the comparison of built-up patterns between years. In Equation 6, X means the value of spatial metrics.

$$X_{standardization} = \frac{X - X_{min}}{X_{max} - X_{min}} \quad \textit{Equation 6}$$

In order to further evaluate the sustainability of urban development in this study area, an indicator named land use efficiency (LUE) (UN-Habitat, 2016) was calculated. In this study, we regard the land consumption as the built-up area derived from land cover/use classification. The land consumption efficiency decreases with the increasing value of LUE. The related equations (Schiavina et al., 2019) are shown below, where BA_i is the area of built-up areas in year i; BA_j means the area of built-up areas in year j; t is the number of years between year i and year j; and P_i represents the population in year i; P_j symbolizes the population in year j; ln is the natural logarithm.

$$LCR = \frac{\ln(BA_i/BA_j)}{t} \quad \textit{Equation 7}$$

$$PGR = \frac{\ln(P_i/P_j)}{t} \quad \textit{Equation 8}$$

$$LUE = \frac{LCR}{PGR} \quad \textit{Equation 9}$$

4. RESULT AND DISCUSSION

In this chapter, the main results achieved in this study are presented and interpreted. Section 4.1 presents the classified maps of the study area and the classification accuracy of each class is assessed. Section 4.2 shows the delineated contiguous built-up areas and the estimated population for each administrative settlement. The urbanizing areas in each year is also identified. Section 4.3 analyses the dynamics of the built-up area and the population changes by interpreting the value of indicators used in this study. Analysis of the urbanization process of the Barharia cluster from a qualitative perspective is also presented in this section. Section 4.4 discusses the results and methods used, as well as the limitations of this study.

4.1. FCN-based land cover/use classification

After several experiments, networks trained for 100 epochs with the learning rate of 0.01 had the best performance for the classification of images in 2005, 2010 and 2018. And as followed by Table 5, the FCN-based land cover/use classification produced reasonable results, with year 2018 and 2010 performing better than year 2005. To be more specific, the classification for the year 2018 and 2010 achieved an F1-score above 84% on all classes, while the classification results of roads in 2005 are not as good as the other two classes. Although the precision of roads in 2005 is 93.2%, the recall is only 29.9%, indicating that many roads were wrongly classified as other classes. There are some possible reasons for this result:
(1) The image in 2005 only has four bands, while the images in 2010 and 2018 have eight bands. Therefore, limited bands may affect the performance of FCN.
(2) There are only a few roads on the image in 2005. Thus, the training samples for roads maybe not enough to allow the FCN to distinguish roads from the other two classes.
(3) Almost no vegetations existed on the ground in the image of June of 2005. Maybe because this is a very dry and hot period as compared to March. Therefore, it is hard to distinguish roads from non-built-up areas due to the similar material and colour of the surface.
Nevertheless, the performance of FCN models on classifying built-up area was rather good in each year. The poor classification accuracy of roads in 2005 did not affect the classification of built-up areas since most of roads are wrongly classified as non-built-up areas. Therefore, the classified maps can be used for built-up area extraction and further identifying urbanizing areas.

Table 5. The performance of FCN for the image in 2018, 2010 and 2005

Year	Class	Precision	Recall	F1-Score
2018	Built-up area	98.7%	97.5%	98.2%
	Road	93.1%	78.9%	84.5%
	Non-built-up area	99.6%	99.7%	99.8%
2010	Built-up area	99.7%	95.6%	97.6%
	Road	83.2%	96.1%	89.1%
	Non-built-up area	99.9%	99.9%	99.9%
2005	Built-up area	98.7%	99.0%	98.8%
	Road	93.2%	29.9%	45.3%
	Non-built-up area	99.3%	99.9%	99.6%

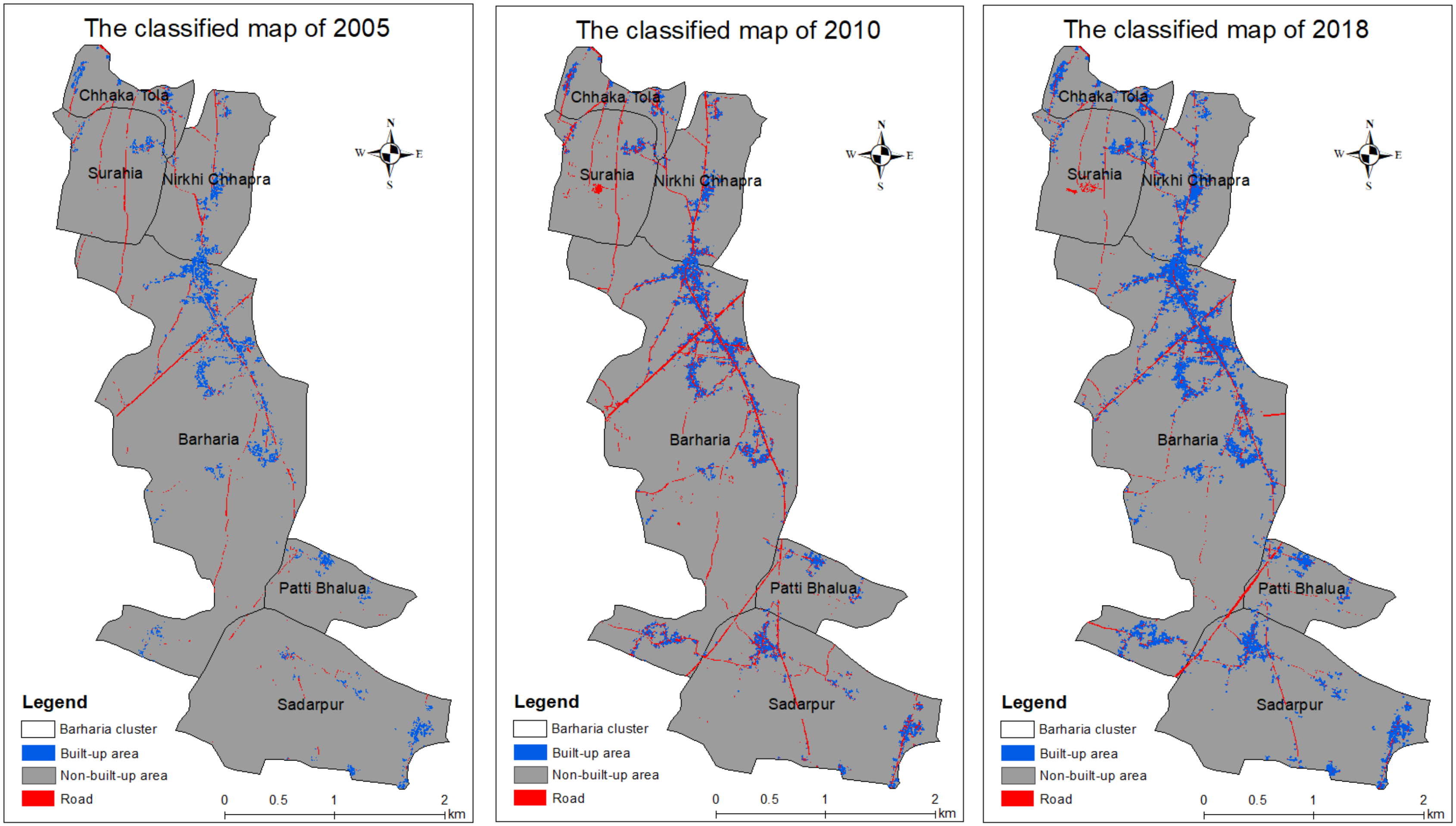

Figure 10. The classified maps of the Barharia cluster for the years 2005, 2010 and 2018

As for the visual inspection of the classified maps (Figure 10), the spatial patterns of land cover/use classes in the study area show that most of the area in the Barharia cluster was non-built-up. The built-up areas were mainly along roads, and the largest part of the built-up area located in the Barharia settlement, which is consistent with the location of urban centre mapped by the GHS-UCD (2019). From 2005 to 2018, the built-up area in each settlement expanded outwards and tended to be close to each other.

4.2. Urbanizing areas delineation

4.2.1. Delineation of contiguous built-up area

For each year, the built-up area is summarized in Figure 11. In all settlements, the size of built-up areas increased between 2005 and 2018. The Barharia settlement contains most of the built-up area, consistent with what we see in the classification maps (Figure 10). And compared with 2005 to 2010, the built-up area increased more distinctly from 2010 to 2018.

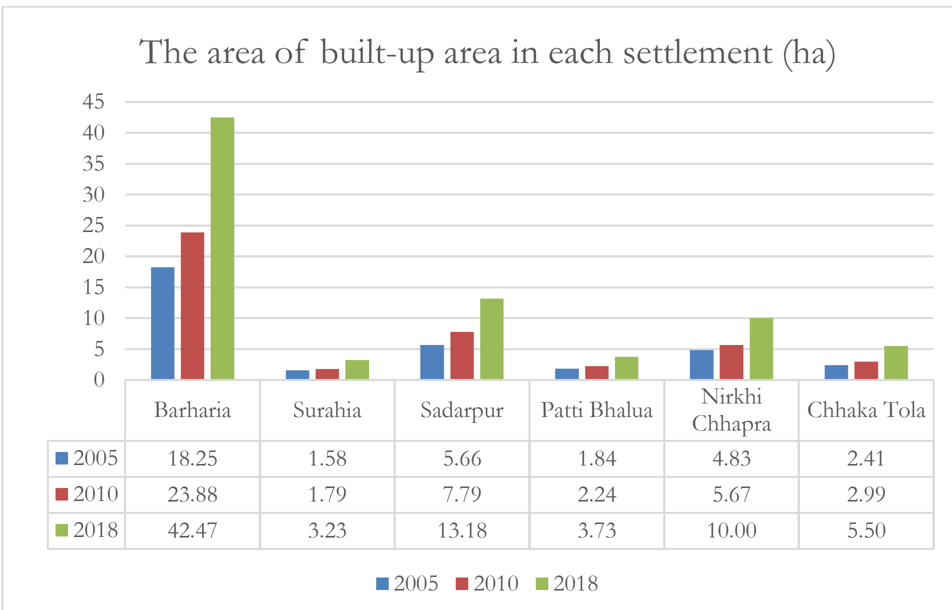

	Barharia	Surahia	Sadarpur	Patti Bhalua	Nirkhi Chhapra	Chhaka Tola
2005	18.25	1.58	5.66	1.84	4.83	2.41
2010	23.88	1.79	7.79	2.24	5.67	2.99
2018	42.47	3.23	13.18	3.73	10.00	5.50

Figure 11. The area of built-up area of each settlement (Unit: ha)

Concerning the contiguous built-up areas in each year, the number of contiguous built-up areas decreased from 2005 to 2018 (seen from Figure 12), since some small and dispersed contiguous built-up areas expanded and aggregated gradually to form a larger contiguous built-up area over time. Besides, some contiguous built-up areas include small built-up areas that are a little bit far away from the main part of the contiguous built-up area. Therefore, some parts of contiguous built-up areas look like branches. Concerning areas covered by clouds in 2005, they were modified to non-built-up areas after the land cover/use classification and were not involved in the population estimation and urbanizing area identification.

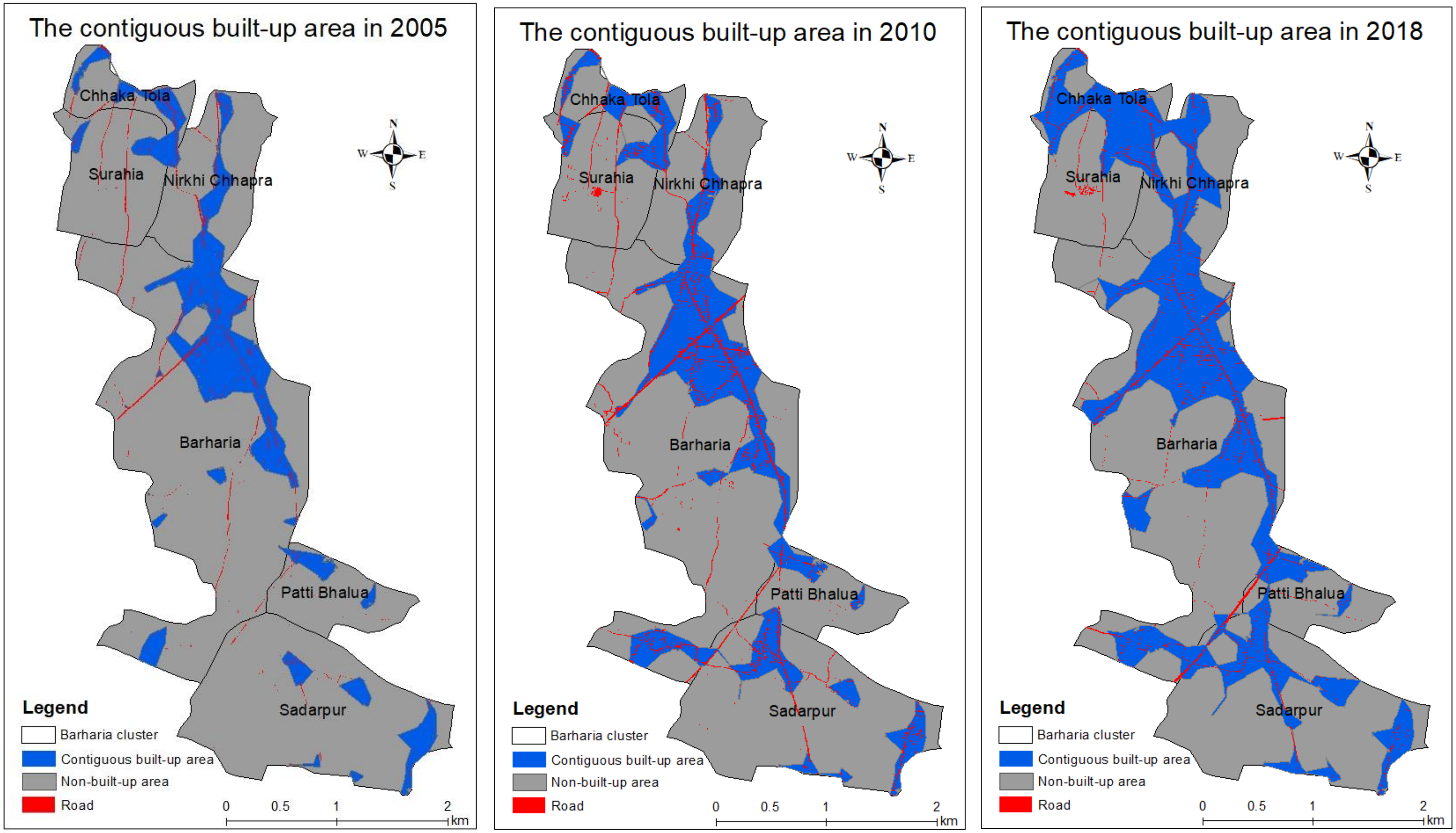

Figure 12. Contiguous built-up areas of the Barharia cluster for the years 2005, 2010 and 2018

4.2.1. Population estimation

Population size and population density of each settlement are presented and compared in this section. The average population growth rate between 2005 and 2018 was 2.3% using Equation 4 and the data of the population Census of the Bihar state in 2001 and 2011. Although the population of Barharia settlement was significantly larger than the other five settlements, the population density of Barharia settlement was penultimate (Figure 13 and 14). Only Nirkhi Chhapra settlement had a population under 1000 people in these three years, and it had the lowest population density. Besides, the population density of Surahia, Sadarpur and Patti Bhalua settlements were similar. And Chhaka Tola settlement, the most northern settlement, had the third-largest population but had the highest population density in 2005, 2010 and 2018.

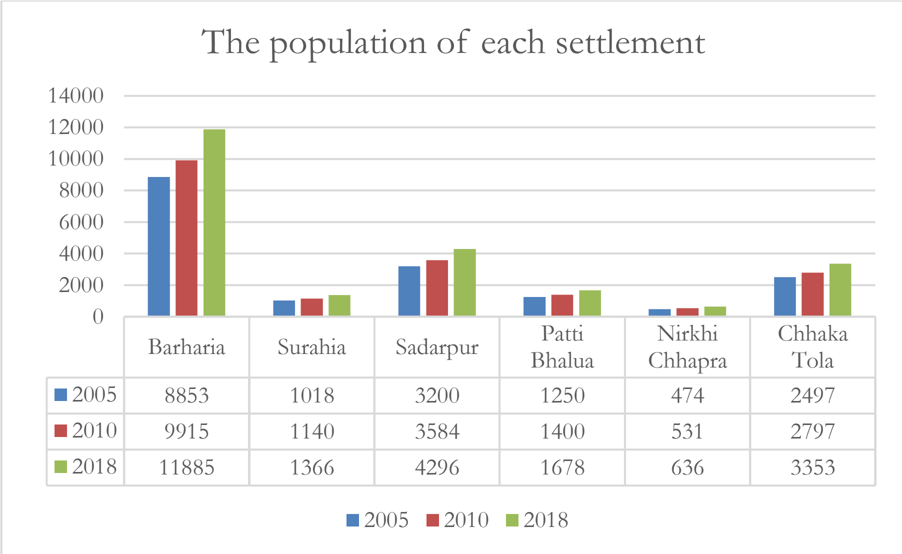

	Barharia	Surahia	Sadarpur	Patti Bhalua	Nirkhi Chhapra	Chhaka Tola
2005	8853	1018	3200	1250	474	2497
2010	9915	1140	3584	1400	531	2797
2018	11885	1366	4296	1678	636	3353

Figure 13. The population of each settlement in 2005, 2010 and 2018 (Unit: number of people)

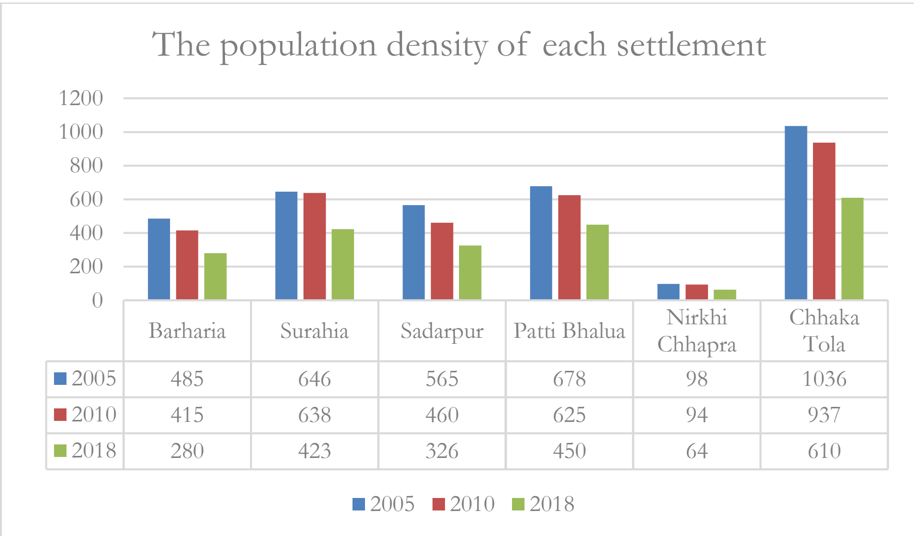

	Barharia	Surahia	Sadarpur	Patti Bhalua	Nirkhi Chhapra	Chhaka Tola
2005	485	646	565	678	98	1036
2010	415	638	460	625	94	937
2018	280	423	326	450	64	610

Figure 14. The population density of each settlement in 2005, 2010 and 2018 (Unit: number of people per ha)

4.2.2. Identification of urbanizing areas

The population and area of all the contiguous built-up areas in each year are listed in Table 6. As we mentioned in section 3.5.2, the population of contiguous built-up areas of Sadarpur settlement in 2005 was not accounted for in this table. From Table 6, we can see that the number of contiguous built-up area is decreasing over time, indicating that the built-up area is aggregating. One third of contiguous built-up areas were less than one ha in 2005. However, all contiguous built-up areas were larger than one ha in 2010 and 2018. According to the definition of the urbanizing area, one contiguous built-up area could be identified as an urbanizing area in 2010 and 2018 respectively (marked as red in Table 6). And there was no urbanizing area in 2005.

Table 6. The number of contiguous built-up area and their areas in each year (urbanizing areas are marked as red; contiguous built-up area 11-15 in 2005 was in Sadarpur, and their population was not estimated.)

Year	Contiguous built-up area	Area (ha)	Population
2018	1	7.12	520
	2	2.27	211
	3	12.68	932
	4	314.62	21550
2010	1	32.56	3961
	2	1.62	130
	3	1.55	196
	4	35.65	3157
	5	4.22	387
	6	3.86	349
	7	11.69	1048
	8	137.44	10135
2005	1	22.38	3227
	2	2.28	310
	3	1.74	173
	4	0.24	24
	5	0.85	84
	6	0.68	68
	7	6.39	1021
	8	1.55	251
	9	5.17	515
	10	99.58	8408
	11	4.25	--
	12	3.95	--
	13	0.97	--
	14	0.76	--
	15	10.76	--

4.3. Urban dynamics analysis

Regarding the urban dynamics trend of this study area, contiguous built-up areas in the Barharia cluster had a tendency of aggregation and the urbanizing area experienced urban expansion between 2010 and 2018. To be more specific, the aggregation process of each contiguous built-up area from 2005 to 2018 is shown in Figure 15. This diagram only presents the number of contiguous built-up areas in each year and their aggregation trajectory, not relating them to the area of each contiguous built-up area. Rectangles with different colours in each year represent different contiguous built-up areas. And contiguous built-up areas of the previous year connected by the same coloured flows were merged into a new contiguous built-up area in the next time stamp. From Figure 15, there were six built-up patches in 2005 where every two merged into one built-up patch in 2010 and five built-up patches in 2005 merged into one dominant built-up patch in 2010. Therefore, the number of built-up patches decreased from fifteen to eight from 2005 to 2010. Besides, except for three built-up patches that had existed since 2005 (which colour remains the same in three years), all built-up patches merged into one big patch in 2018, and the number of built-up patches decreased from eight to four from 2010 to 2018. Combining with Figure 12, we can see that all built-up patches themselves were expanding, and the dominant built-up patch kept absorbing the surrounding built-up patches from 2005 to 2018.

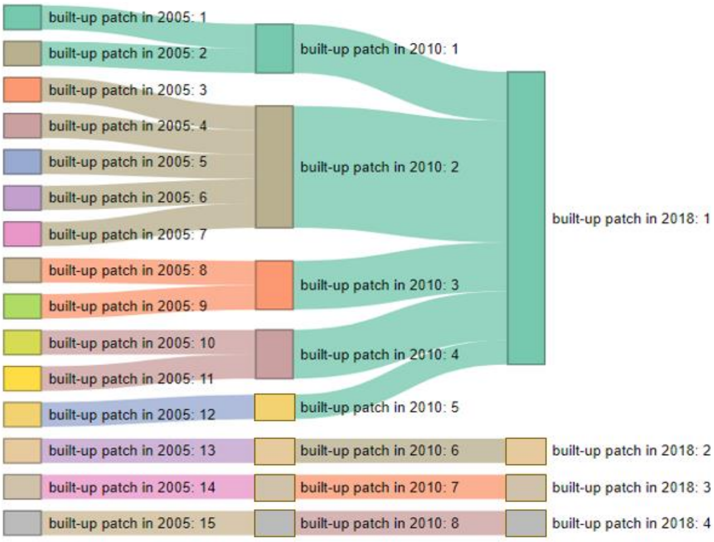

Figure 15. Sankey diagram of the aggregation process of contiguous built-up areas

This study also analyses the spatial pattern of contiguous built-up areas. From the visual inspection of Figure12, contiguous built-up areas were relatively small and dispersed in 2005 compared with the other two years. When it comes to 2010, contiguous built-up areas in each settlement expanded outwards since 2005, and a part of contiguous built-up areas in the Patti Bhalua settlement was included in the largest contiguous built-up area. From 2010 to 2018, contiguous built-up areas continued to expand, and the largest contiguous built-up area included built-up areas in all settlements. Besides, the main part of the largest contiguous built-up area is located in the Barharia and Nirkhi Chhapra settlements from 2005 to 2018.

As indicated in section 3.6, the spatial dynamics of the Barharia cluster was quantitatively analysed from three aspects, namely built-up area morphology change, urbanizing areal extent change and population change. Indicators related to morphological analysis of contiguous built-up areas are standardized and shown in Figure 14. The increase of built-up density from 2005 to 2018 shows that built-up areas expanded over time. And a decreasing number of patches together with the increase of AI over time, indicates that built-up patches have a trend of aggregation. Besides, built-up areas become more aggregated, resulting in a significant growth of the largest built-up patch from 2010 to 2018. The average minimum distance between patches grew significantly from 2010 to 2018 because most of built-up areas have formed a contiguous built-up area, and the rest of built-up areas are relatively farther away and more isolated.

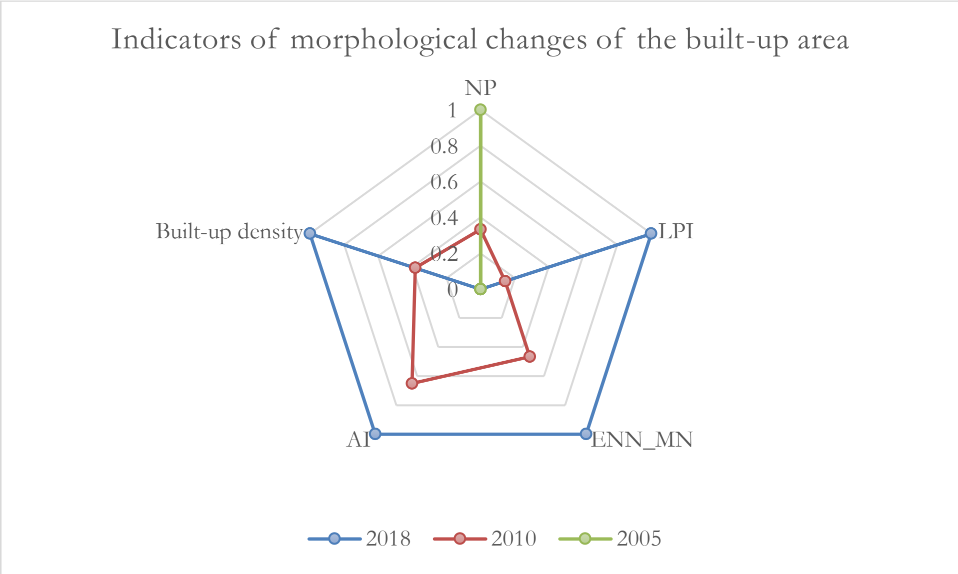

Figure 16. The radar chart of indicators of built-up area morphology changes in the Barharia cluster

As for the population and urban areal extent change, according to Table 7, the population density decreased from 2010 to 2018, though the population doubled in eight years, according to the estimates. Combined with the LUE of the Barharia cluster, which is 2.2 from 2005 to 2010 and 3.1 between 2010 and 2018, this result shows that the growth rate of built-up area was larger than the growth rate of population and the land consumption efficiency decreased from 2005 to 2018. Moreover, about only half of the population (52.33%) lived in urbanizing areas in 2010, while it increased to 92.83% in 2018, showing that the percentage of people living in urbanizing areas increased significantly (about 40%) in eight years.

Table 7. Indicators of urban dynamics analysis

Factors	Indicators	2005	2010	2018
Urbanizing areal extent change	The areal extent of urbanizing areas (ha)	0	137.44	314.62
Population change	Population density of urbanizing areas (per ha)	0	74	69
	The total population of urbanizing areas	0	10135	21550
	The proportion of population in urbanizing areas compared with the whole cluster	0	52.33%	92.83%

When we zoom in to the population in urbanizing areas in each administrative settlement (Figure 17), as we indicated before, only three settlements had an urbanizing population in 2010, and it increased to six in 2018. Because built-up areas in Surahia, Sadarpur and Chhaka Tola settlements were not included in urbanizing areas in 2010, but all of them were subsumed in the urbanizing area in 2018 due to the aggregation of built-up areas.

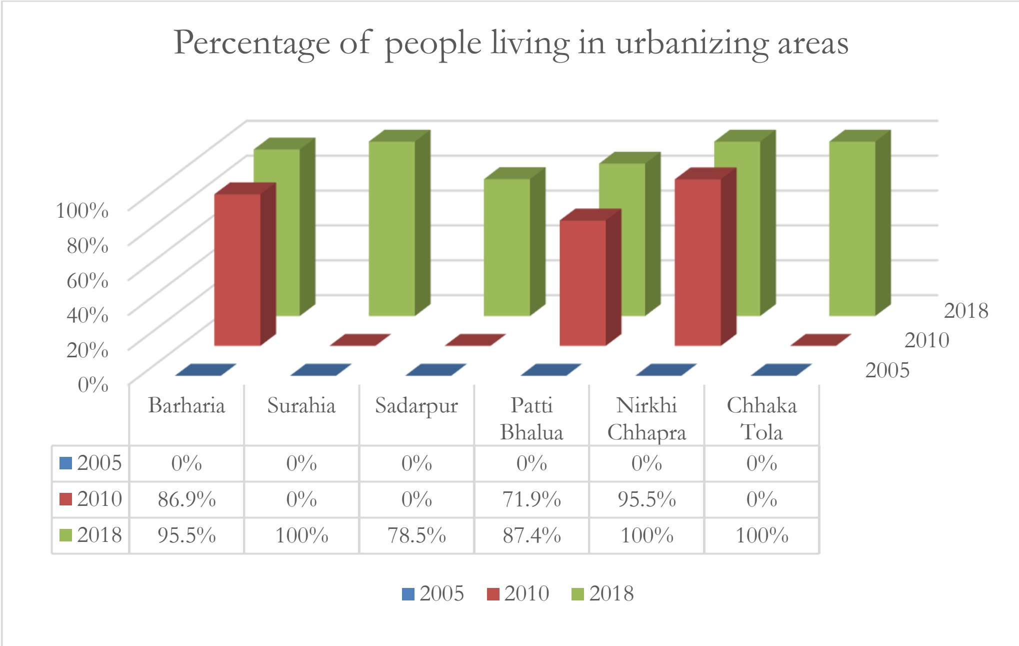

	Barharia	Surahia	Sadarpur	Patti Bhalua	Nirkhi Chhapra	Chhaka Tola
2005	0%	0%	0%	0%	0%	0%
2010	86.9%	0%	0%	71.9%	95.5%	0%
2018	95.5%	100%	78.5%	87.4%	100%	100%

Figure 17. The percentage of people living in urbanizing areas

Moreover, the urbanization process of the Barharia cluster is also analysed from a qualitative perspective. Satellite images of an area located in the northern Barharia settlement are displayed as an example in Figure 18. Figure 18(a), (c) and (e) were satellite images captured in 2005, 2010 and 2018 respectively. Figure 18(b), (d) and (f) are part of Figure 18(a), (c) and (e), the former three showing buildings clearly. In 2010 and 2018, the main roads on the right part of Figure 18(c) and (e) were improved, compared with the corresponding road in 2005. Besides, from 2005 to 2018, buildings in this area became larger and denser, new buildings were mainly built along roads or upgraded in situ (examples are marked as red circles in Figure 18(b), (d) and (f)). The improvement of buildings and roads suggests an increasing income and better quality of life of local people with the development of urbanizing areas.

(a) (b)

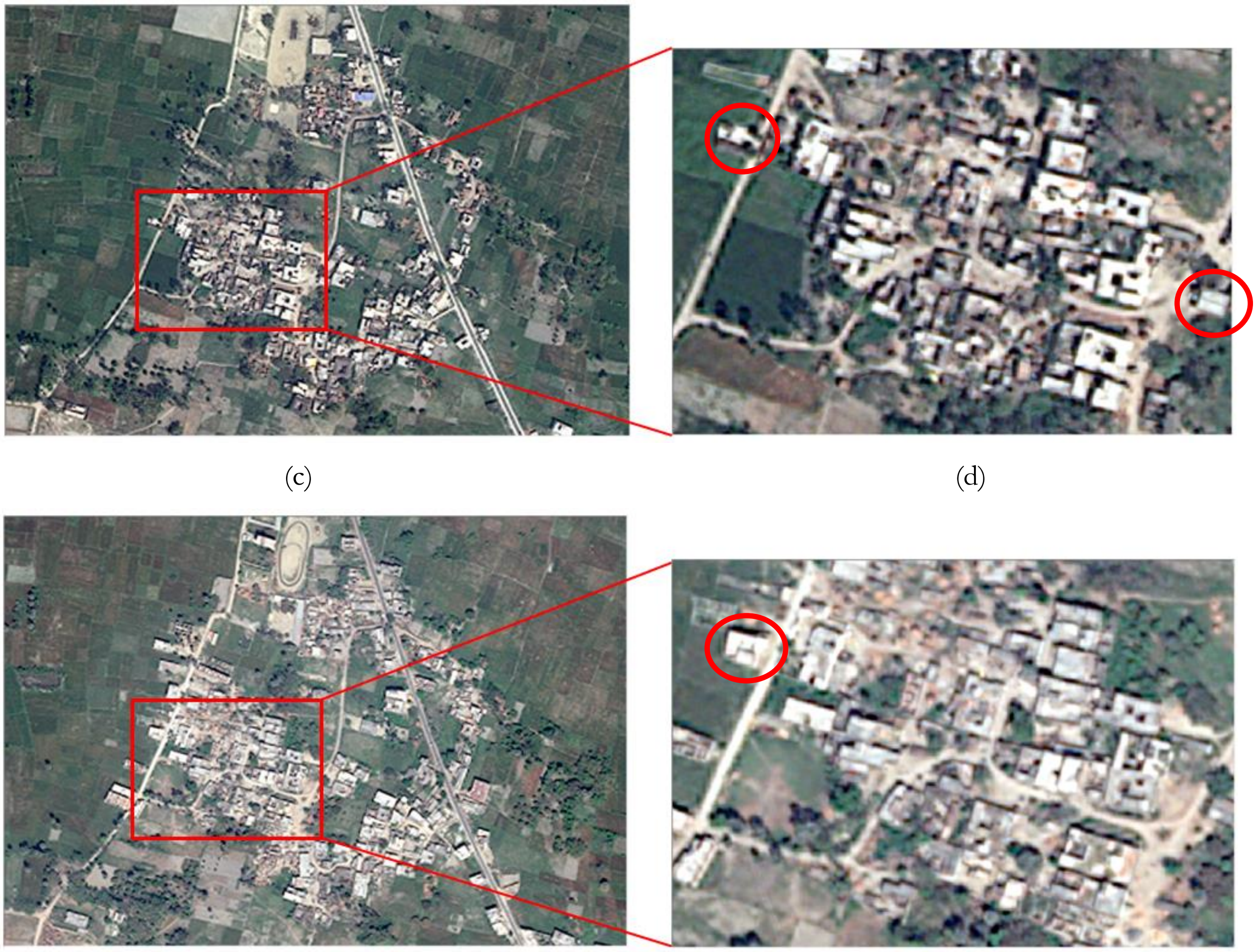

(c) (d)

(e) (f)

Figure 18. Changes of buildings and roads from 2005 to 2018(Data source: WorldView-2 image in 2018)

4.4. Discussion and limitation

4.4.1. Land cover/use classification using FCN

In this study, given the limited availability of detailed reference data, three classes (built-up areas, roads, and non-built-up areas) were selected to describe the dynamics of urbanizing areas and were classified from VHR satellite images. Here built-up areas were classified for the generation of contiguous built-up areas, and the classified roads served as a spatial reference to trace the trajectory of the built-up area expansion. The rest of land cover/use types which are out of the interest in this study were included in the class of non-built-up areas. Although these three classes can help to capture urbanizing areas and the urbanization trends, a more detailed classification on different building types, such as houses with different qualities, could further reflect socio-economic conditions and contribute to generating information about social and economic transformations. However, for this study, the available datasets were not of sufficient detail to support the classification of different building types; this limitation and details of buildings existed in the study area is further elaborated in section 4.4.4. And the explicit definition of different housing types needs to be put forward carefully based on information obtained by related fieldworks.

The data pre-processing strategy for the image classification was formulated according to the context of the study area. In principle, selected training and testing tiles used for training FCNs are required to cover all classes and the FCNs needed to be fed by enough labelled samples to ensure the training and testing accuracy. In this study, we selected tiles that covered most of the area of interest (built-up areas) and created reference maps by visual interpretation. This strategy is suitable for land cover/use classification based on remote sensing images in relatively small regions. However, if multiple datasets are available for training and they are in good quality, one more rule needs to be added to the tile selection strategy, which is to select tiles that are covered by different datasets as many as possible. While many open-source datasets are available nowadays, their quality cannot be guaranteed in rural areas (Mahabir, Stefanidis, Croitoru, Crooks, & Agouris, 2017). Lack of suitable data sources is a problem that restricts the exploration of suitable data preparation strategy in this study and this limitation is also discussed in section 4.4.4.

Furthermore, FCNs can be used for land cover/use classification at various geographic scales. Most of the studies applied FCNs to do land cover/use classification at the city level (e.g., Zhang, Wei, Ji, & Lu, 2019) or specific regions of interest, while some researchers such as He et al. (2019) classified urban and non-urban areas at the global level based on a variety of datasets. Besides, Tan et al. (2019) classified built-up areas and non-built-up areas from 32 regions in China based on VHR panchromatic images using FCN and achieved high testing accuracy (98.75%), showing the transferability of FCNs.

When it comes to the accuracy assessment of land cover/use classification, first, the boundaries of built-up areas and roads in classified maps can be fuzzy, compared with the reference maps and input images. Second, from a quantitative perspective, this study adopted criteria related to the confusion matrix to assess the classification accuracy of FCNs, which are commonly used in many studies (Fu et al., 2017; Yang, Zhuang, Bi, Shi, & Xie, 2017). However, this accuracy assessment approach highly relies on the accuracy of the ground truth data and the matching degree between the classification results and the ground truth data (Foody, 2002). We cannot know the location of wrongly classified pixels from the confusion matrix. This study manually delineated polygons representing each class and converted these polygons to raster, which has the same pixel size as the training and testing tiles to create reference maps. Therefore, there may be errors occurring at the edge of polygons in the conversion process. Besides, there were uncertainties in the calculation of indices because not all pixels in reference maps are labelled. However, this study labelled about 70 to 80 per cent of pixels in reference maps and we believed that it is enough to evaluate the performance of FCNs. When it comes to create training samples for areas at a large scale, Tan et al. (2019) labelled built-up areas at a block level. They manually selected blocks with 64 by 64 pixels and regarded blocks with more than 50% of the built-up area as training samples. This is a time-saving method for binary classification, but its feasibility on multi-class classification needs to be tested.

4.4.2. Delineation of urbanizing areas

This study delineated contiguous built-up areas based on classified maps using the aggregation tool. However, there were some 'noises' (a small group or isolated pixels that are wrongly classified as other classes) in the classified maps. Some studies removed noises at the pixel level based on methods such as the Majority Analysis or Classification Clumping (Liu et al., 2019). However, in this study, we removed these noises by selecting 'built-up' polygons that meet our criteria. One reason is that using these pixel-based methods may further smoothen built-up areas. Besides, we mainly use 'built-up' polygons instead of pixels for further analysis. Therefore, removing tiny 'built-up' polygons is, in our opinion, a more suitable option. Also, the aggregation tool used in this study partly kept the original edges of built-up areas. Therefore, the shape of the derived continuous built-up area is closer to the actual shape than the built-up area generated by the regular polygon mosaic (for example, the city centre shown in Figure 19).

With regard to the method for census data disaggregation, we assume that the population of one contiguous built-up area is proportional to its area. This assumption can only help us roughly estimate the population of continuous built-up areas and identify urbanizing areas, achieving the sub-objective of this study. But the detailed population distribution within urbanizing areas, which to some extent reflects the social-economic activities of residents, cannot be obtained. The limitation of the methods and datasets used for population estimation and census data disaggregation is further discussed in section 4.4.4. We applied a top-down population estimation method in this study, while some studies estimated population using bottom-up methods. For instance, Weber et al. (2018) estimated the population density of regions in northern Nigeria, based on the small-scale census conducted by a local non-government organization and the area of residential areas classified by VHR images. They got a more detailed population distribution than the information provided by census data. The population estimated using the bottom-up method is more in line with the actual situation, especially for regions with inadequate geographic information (Weber et al., 2018).

When comparing urbanizing areas in 2018 delineated in this study and the urban centre published by the GHS-UCD (2019), as can be seen from Figure 19, urbanizing areas obtained in this study shows more details in terms of the spatial pattern, while the urban centre from GHS-UCD only covered the central part of urbanizing areas in the Barharia settlement. As we mentioned in chapter 2, GHS-UCD is more suitable to present urban centres of large cities at the global level. When it comes to regions at a smaller scale like this study area, methods as used in this study can better visualize the shape and distribution of urban areas, contributing to urbanization research targeting at small regions.

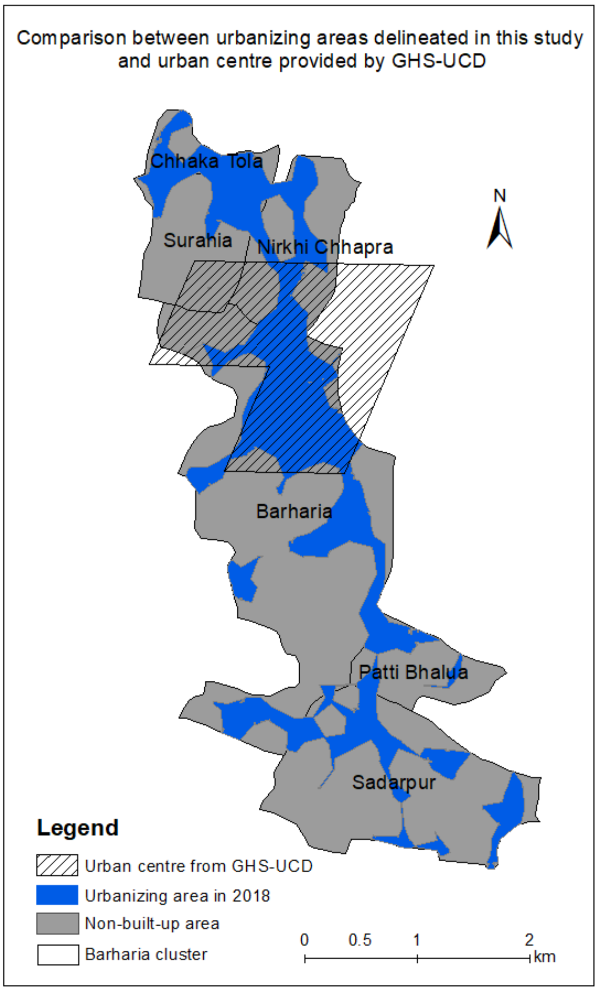

Figure 19. Comparison between urbanizing areas in 2018 delineated in this study and the urban centre published by the GHS-UCD (Data source: the GHS Urban Centre Database (2019))

Theoretically, the definition of contiguous built-up areas and approaches for creating contiguous built-up areas in this study can both be applied at the country level and the global level. But it requires images with high resolution which are normally expensive, and the computational cost is considerable. Therefore, in practical terms, this approach is more suitable for semi-automatically delineating built-up areas in the region of interest to researchers and planners. And products created by applying this approach can be regarded as a supplement to the large-scale global urbanized areas.

4.4.3. Analysis of the urbanization process of the study area

As for the morphological changes of the contiguous built-up area, we found that these areas tended to aggregate together to form larger continuous built-up patches over time. Some cities in their early stage of development, such as Bengaluru and Ahmadabad in India, also had this dynamic, i.e., to absorb surrounding built-up areas for their expansion (Taubenböck et al., 2009). And some cities in another developing country, China, have the same growth trend of built-up areas with the Barharia cluster. Dongguan, which locates in the southern China, experienced a conversion from a small city dominated by a small largest patch in 1975, to a large agglomeration consisting of a quite large patch surrounded by many small patches in 2010, and the built-up area of Shenzhen had the same growing progress with Dongguan between 1975 and 2010 (Taubenböck et al., 2019). During this period, patches in Dongguan and Shenzhen constantly added and aggregated with each other, and finally formed a large city. We could imagine that this study area is possibly to become a large agglomeration in the future, but it also depends on many other factors such as the local economic development.

When it comes to population changes, the population density in this study area decreased from 2010 to 2018. According to research developed by Terfa et al. (2019), Addis Ababa, Ethiopia and Arua, Uganda experienced the same decrease trend of population density with the Barharia cluster. One possible reason is that this study area is a newly emergent urbanizing area with sufficient vacant land for urban development. And with the increase in income, local residents had improved their living environment, such as upgrading their houses.

We also notice that the land consumption efficiency of the Barharia cluster deceased from 2005 to 2018, indicating that the development of this study area runs counter to the Goal 11 of SDGs (mentioned in section 1.1). Schiavina et al.(2019) calculated the LUE for different types of settlements based on the definition of urban provided by European Commission (2019), showing that the LUE of urban centres and urban clusters between 1990 and 2015 is around 1, while the LUE of rural area is about 2. Besides, about half of the urban centre in the world has the LUE between 0 and 1(Schiavina et al., 2019), which is a relatively good range, indicating a more compact urban area, since the growth rate of population is larger than that of land consumption. Therefore, the land consumption efficiency of this study area is quite low compared with other cities (2.2 between 2005 and 2010; and 3.1 between 2010 and 2018). Planners should be aware of this situation and guide this region towards a sustainable development.

As we mentioned in section 3.1, this study area shows great potential to have urbanizing areas that are ignored by the government. Combining the observation from the morphological changes of built-up area and population changes, we confirmed that an urbanizing area emerged and kept growing between 2010 and 2018. The urbanization process of many other rural areas in the Bihar state are also hidden and the reasons for this phenomenon are multiple. Bihar has the highest growth rate of people living in rural areas engaging in non-farm works between 2000 and 2015, compared with other states in India, which seems to promote the urbanization process of the rural area (Van Duijne, 2019). Some cities tend to absorb surrounding rural areas where the majority of people doing non-farm works to expand the size of the city and therefore get more budget for urban development such as improving public facilities. However, according to the study of Van Duijne (2019) in Samastipur, a small city in Bihar, the following factors hindered the administrative integration between regions:

1) Integrating into the city will bring uncertainty to local land ownership and affect households engaging in farm works.

2) Areas certified as rural can receive state-subsidized rural development funds.

3) People in rural areas worry that the living cost will increase after being incorporated into the city.

4) People in rural areas do not trust the city government and becoming a part of the city will reduce their participation in political activities.

In all, the conflict of interest between people in the city and the rural area makes it difficult for the urbanizing villages to administratively becoming a part of the city, which in turn causes the urbanization process in these areas to be hidden. In this study, administratively aggregating these villages to form a new city may also face the same obstacle.

4.4.4. Limitation

First, the satellite image of 2005 does not cover the whole study area and contains some clouds, hindering the extraction of built-up areas and the estimation of population. Besides, as we mentioned in section 4.1, the image in 2005 was acquired in March and there are only a few areas covered by vegetation. This could be a reason of the low classification accuracy of roads. In this study, satellite images are the only data source for land cover/use classification. One reason is that VHR images in the Global South is not easy to obtain, and open-source dataset such as open street maps are normally not accurate in small regions (Aguilar & Kuffer, 2020). This limitation hinders the attempt of doing more detailed land cover/use classification in this study.

We only classified three land cover/use classes in this study. It would be interesting to classify classes representing different types of buildings based on diverse data sources. According to data collected in the field by Doctor candidate Van Duijne from the University of Amsterdam, there are three kinds of houses: pucca houses, semi-pucca houses and kutcha houses (shown in Figure 20). It is difficult to distinguish these kinds of houses from the dataset we have. Analysing changes of different types of houses over time can help analyse the house upgrading of urbanizing areas. Therefore, the classification of different types of houses through machine learning algorithms based on multiple datasets is a direction deserving further research. Some datasets are recommended, such as images captured by unmanned aerial vehicles (UAVs) with the resolution at centimetre level, which can better describe characteristics of houses. For instance, Gevaert, Persello, Sliuzas and Vosselman (2017) classified informal settlements (which normally consist of buildings with irregular shapes and blended material of roofs) based on images obtained by UAVs successfully, with an accuracy of larger than 90% in Rwanda and Uruguay. And social-economic data like the household size and the income of family members may also be useful datasets to help distinguishing different type of houses. Nevertheless, the geo-location of surveyed households needs to be very precise then.

(a) (b) (c)

Figure 20. Examples of different types of buildings in the Barharia cluster ((a): pucca house; (b): semi-pucca house; (c): kutcha house; Source: photographs are provided by PhD candidate Van Duijne, R. J., the University of Amsterdam, obtained during the fieldwork in the Barharia cluster in 2018)

A second limitation refers to the population estimation and disaggregation. Population estimation of each settlement was only based on the census data of the Bihar state in 2001 and 2011. There is uncertainty about the real population growth rate after 2011. It is better to add more data sources such as a household survey to better estimate the population in the study area. There are also uncertainties in the census data due to multiple reasons. One reason is that some residents are sceptical about the official survey and do not cooperate with the collection of demographic information (Srivastava, 1972). This leads to an omission of population in entire India, with 23 per 1000 people and the omission in the eastern India (where the study area located in) is slightly lower, 20 per 1000 people, in the census data of 2011 (Indian Census Bureau, 2011).

As for the methods used for disaggregating population of each settlement, the assumption of the distribution of population on built-up areas is simpler compared with studies mentioned in section 2.3 because we do not have additional dataset like the night-time light data or detailed land use maps to further disaggregate the population of administrative units. Also, current free night-time light datasets normally have coarse resolution with hundreds of metres which is not suitable for small regions (Zhao et al., 2019). Further studies could estimate the population of small regions at a more detailed level based on local social-economic data or surveys from fieldworks. The population distribution can be used to compare the changes of population density in the city fringe with the population density in the city centre to better describe the migration of people in the process of urban development and to better understand the formation of urban areas in small regions.

5. CONCLUSION AND RECOMMENDATION

The objective of this study was to generate an FCN-based approach to analyse the spatial dynamics of urbanizing areas in a semi-automatic way. Some urbanizing areas exist in officially defined rural regions, but are ignored by the government, hindering the understanding of the real urbanization process. Therefore, it is necessary to detect the unseen urbanizing areas, not only providing spatial information for the study of urban forms, but also helping planners to carry out regional profiles and support targeted policy making. To achieve this general objective, three sub-objectives were accomplished by answering related research questions in this study.

First, classified maps were obtained by training FCN based on VHR satellite images. Built-up areas, roads and non-built-up areas were classified in 2005, 2010 and 2018 for the Barharia cluster. Built-up areas were the focus of this study and were further used to identify urbanizing areas. Roads contributed to the spatial analysis of the expansion of built-up areas. Thirteen tiles in 2010 and 2018 and eleven tiles in 2005 were selected following the tile selection strategy and corresponding reference maps were also generated by visual interpretation. Besides, FCN architecture developed by Persello and Stein (2017) was adopted to classify the three classes. As for the classification accuracy, the performance of FCN models was assessed by indices related to the confusion matrix. All classes in 2010 and 2018 were classified well, with the F1-score above 84%, while many roads were wrongly classified as other classes (mostly non-built-up areas), with the recall of only 30%. However, the built-up areas in 2005 were well classified. Therefore, classified built-up areas in these three years both can be used to further generate contiguous built-up areas and identify urbanizing areas. The built-up areas of the Barharia cluster increased from 34.57 ha in 2005 to 87.11 ha in 2018.

Second, urbanizing areas were identified in this study. Here we adopted the definition of urbanizing areas proposed by Denis and Marius-Gnanou (2010). To delineate urbanizing areas, first, built-up areas under 15 square metres were removed to reduce the noises in classification results. And then, polygons representing built-up areas were aggregated together to form contiguous built-up areas. Meanwhile, we estimated the population growth rate of 2.3% in the study area between 2005 and 2018 based on the census data of Bihar in 2001 and 2011. The population of each administrative settlements in each year was also estimated and was used for the estimation of the population in each contiguous built-up area. According to the urbanizing area definition, the Barharia cluster contained one urbanizing area in 2010 and 2018 respectively and there was no urbanizing area in 2005.

As for the spatial dynamic analysis of urbanizing areas in the study area, in general, the contiguous built-up areas had a trend of aggregation and contiguous built-up areas expanded from 2005 to 2018. To be more specific, the number of contiguous built-up areas decreased over time and these built-up areas tend to aggregate to form new contiguous built-up areas. From the classified maps and the distribution of contiguous built-up areas, we can see that many newly emergent built-up areas were located along roads and these built-up areas connected contiguous built-up areas to form a larger one. The largest contiguous built-up area in 2010 expanded itself by self-growing and absorbing surrounding built-up areas, forming an urbanizing area with 137.44 ha and 10135 population. From 2010 to 2018, the urbanizing area kept expanding and covered all administrative settlements, with 314.62 ha and 21550 population. When it comes to the population change in urbanizing areas, only half of the total population lived in urbanizing areas in 2010, while this proportion came to 92.83% in 2018. And the total population in the urbanizing area doubled in eight years. Compared with the urbanization process of other cities in the world such as Dongguan (Taubenböck et al., 2019) from the growth trend of urbanizing areas, this study area has the possibility to develop into a big agglomeration in the future.

The approach provided in this study can help researchers depict urbanizing areas more efficiently compared with manual delineation and contribute to the analysis of hidden urbanization process in small regions. Supported by related literature (Van Duijne, 2019), the conflict of interest between governments of cities and rural residents, especially those engaged in agricultural works, is the main reason that prevents the administrative integration of urbanizing areas into cities. Researchers and policy makers should be aware of and understand the urbanization process in small regions that has been neglected. Furthermore, policies need to be formulated to help mitigate the conflict not only between cities and surrounding villages, but also between villages that have a tendency to form new cities.

Denis and Marius-Gnanou (2010) manually delineated the contiguous built-up area from satellite images such as Ikonos. In this study, this process was automated by the combination of FCN image classification and aggregation tool. The method used in this study is more time efficient and more suitable for high-volume and repeatable production, but it may not be suitable for a very large area due to the computational cost and the availability of VHR images.

5.1. Recommendation

Some recommended research directions for further study are listed in this section:

1. Exploring an approach to classify different types of buildings in villages.

   In this study, we only classified built-up areas and other two classes from images. Classifying different types of buildings based on multiple data sources to interpret the upgrade process of housing deserves further exploration.

2. Generating methods to estimate and disaggregate population of small regions.

   Most of the studies related to population estimation and disaggregation focus on large cities. And the method used in this study to disaggregate population in small regions is only based on simple assumptions. Based on the advantages shown in the research of Weber et al. (2018), it would be a good direction to explore bottom-up methods estimating and discretizing the population of small areas more precisely.

3. Doing researches related to urban development of small regions through the collaboration between geo-spatial scientists and urban studies scholars.

   The study area was targeted by PhD candidate Van Duijne after doing social-economic analysis for this region. And we identified urbanizing areas from this area, contributing to his research on urban form. This provides an inspiration for the cooperation of geo-spatial scientists and urban studies scholars on comprehensively analysing urban dynamics of small areas. Because urban study scholars could analyse the urban development of small areas from the socio-economic aspect, and geo-spatial experts could provide detailed spatial information on areas of interest.

4. Providing spatial information on urbanizing areas at national wide and put forward proper policies to guide the development of newly emergent urbanizing areas.

   In this study, we found urbanizing areas that were ignored by the government in India, and it is most likely not the only case. Therefore, it is a good direction to produce comprehensive spatial information on urbanizing areas at national wide, helping researchers and planners better understand the urbanization process in small regions. And as elaborated in section 4.4.3, it is possible to have some social and economic related reasons that hinders the administrative aggregation between villages which containing urbanizing areas. Therefore, targeted policies that encourage the integration of urbanizing areas also deserve further research.

LIST OF REFERENCES

A New Urban Epoch? Alternative ways to measure urbanization using VHR remote sensing data. (n.d.). Retrieved from https://www.nwo.nl/en/research-and-results/research-projects/i/83/26983.html

Aguilar, R., & Kuffer, M. (2020). Cloud Computation Using High-Resolution Images for Improving the SDG Indicator on Open Spaces. *Remote Sensing*, *12*(7), 1144. https://doi.org/10.3390/rs12071144

Balk, D. L., Deichmann, U., Yetman, G., Pozzi, F., Hay, S. I., & Nelson, A. (2006). Determining Global Population Distribution: Methods, Applications and Data. *Advances in Parasitology*, Vol. 62, pp. 119–156. https://doi.org/10.1016/S0065-308X(05)62004-0

Bergado, J. R., Persello, C., & Gevaert, C. (2016). A deep learning approach to the classification of sub-decimetre resolution aerial images. *International Geoscience and Remote Sensing Symposium (IGARSS)*, 1516–1519. https://doi.org/10.1109/IGARSS.2016.7729387

Bertaud, A. (2001). Metropolis :A Measure of the Spatial Organization of 7 Large Cities. Retrieved from http://alain-bertaud.com/images/AB_Metropolis_Spatial_Organization.pdf

Brenner, N., & Schmid, C. (2014). The 'Urban Age' in Question. *International Journal of Urban and Regional Research*, *38*(3), 731–755. https://doi.org/10.1111/1468-2427.12115

Champion, T., Hugo, G., & Zhu, Y. (2018). Changing Urbanization Processes and In Situ Rural-Urban Transformation: Reflections on China's Settlement Definitions. *New Forms of Urbanization* (pp. 207–228). https://doi.org/10.4324/9781315248073-11

Chen, Y., Lin, Y., Kung, C., Chung, M., & Yen, I. (2019). Design and Implementation of Cloud Analytics-Assisted Smart Power Meters Considering Advanced Artificial Intelligence as Edge Analytics in Demand-Side Management for Smart Homes. *Sensors*, *19*(9), 2047. https://doi.org/10.3390/s19092047

Da Costa, J. N., Calka, B., & Bielecka, E. (2017). *Uncertainty Quantification of the Global Rural-Urban Mapping Project over Polish Census Data.* Paper presented at 10th International Conference on Environmental Engineering, ICEE 2017. https://doi.org/10.3846/enviro.2017.221

Denis, E., & Marius-Gnanou, K. (2010). Toward a better appraisal of urbanization in India. *Cybergeo*. https://doi.org/10.4000/cybergeo.24798

Denis, E., Mukhopadhyay, P., & Zérah, M. H. (2017). Subaltern Urbanisation in India. *Economic and Political Weekly*. https://doi.org/10.1007/978-81-322-3616-0

Dunn, C. P., Sharpe, D. M., Guntenspergen, G. R., Stearns, F., & Yang, Z. (1991). *Methods for Analyzing Temporal Changes in Landscape Pattern*. 173–198. https://doi.org/10.1007/978-1-4757-4244-2_8

Dutta, I., & Das, A. (2019). Application of geo-spatial indices for detection of growth dynamics and forms of expansion in English Bazar Urban Agglomeration, West Bengal. *Journal of Urban Management*, *8*(2), 288–302. https://doi.org/10.1016/j.jum.2019.03.007

Ellman, T. (1997). Infill: The Cure for Sprawl? . *Arizona Issue Analysis*, 146. The Goldwater Institute. Retrieved from https://www.yumpu.com/en/document/view/5490958/infill-the-cure-for-sprawl-goldwater-institute

Esch, T., Bachofer, F., Heldens, W., Hirner, A., Marconcini, M., Palacios-Lopez, D., … Gorelick, N. (2018). Where We Live—A Summary of the Achievements and Planned Evolution of the Global Urban Footprint. *Remote Sensing*, *10*(6), 895. https://doi.org/10.3390/rs10060895

Foody, G. M. (2002). Status of land cover classification accuracy assessment. *Remote Sensing of Environment*, Vol. 80, pp. 185–201. https://doi.org/10.1016/S0034-4257(01)00295-4

Freire, S., Aubrecht, C., & Wegscheider, S. (2011). S*patio-Temporal Population Distribution and Evacuation Modeling for Improving Tsunami Risk Assessment in the Lisbon Metropolitan Area.* Paper presented at Gi4DM 2011, Turkey. Retrieved from https://www.isprs.org/proceedings/2011/Gi4DM/PDF/OP32.pdf

Fu, G., Liu, C., Zhou, R., Sun, T., & Zhang, Q. (2017). Classification for High Resolution Remote Sensing Imagery Using a Fully Convolutional Network. *Remote Sensing*, *9*(5), 498.

https://doi.org/10.3390/rs9050498
Indian Census Bureau. (2011). Post enumeration survey reports. Retrieved from https://censusindia.gov.in/2011Census/pes/pes_highlights.html
Geopolis | E-Geopolis Institute. (n.d.). Retrieved from http://e-geopolis.org/le-projet/geopolis/
Gevaert, C. M., Persello, C., Sliuzas, R., & Vosselman, G. (2017). Informal settlement classification using point-cloud and image-based features from UAV data. *ISPRS Journal of Photogrammetry and Remote Sensing*, *125*, 225–236. https://doi.org/10.1016/j.isprsjprs.2017.01.017
Gislason, P. O., Benediktsson, J. A., & Sveinsson, J. R. (2006). Random forests for land cover classification. *Pattern Recognition Letters*, *27*(4), 294–300. https://doi.org/10.1016/j.patrec.2005.08.011
European Commission. (2019). Urban Centre Database UCDB R2019A. Retrieved from https://ghsl.jrc.ec.europa.eu/ghs_stat_ucdb2015mt_r2019a.php
Grippa, T., Linard, C., Lennert, M., Georganos, S., Mboga, N., Vanhuysse, S., … Wolff, E. (2019). Improving Urban Population Distribution Models with Very-High Resolution Satellite Information. *Data*, *4*(1), 13. https://doi.org/10.3390/data4010013
Gustafson, E. J. (1998). Quantifying landscape spatial pattern: What is the state of the art? *Ecosystems*, Vol. 1, pp. 143–156. https://doi.org/10.1007/s100219900011
He, C., Liu, Z., Gou, S., Zhang, Q., Zhang, J., & Xu, L. (2019). Detecting global urban expansion over the last three decades using a fully convolutional network. *Environmental Research Letters*, *14*(3). https://doi.org/10.1088/1748-9326/aaf936
Ji, C., Liu, Q., Sun, D., Wang, S., Lin, P., & Li, X. (2001). Monitoring urban expansion with remote sensing in China. *International Journal of Remote Sensing*, *22*(8), 1441–1455. https://doi.org/10.1080/01431160117207
Liu, R., Kuffer, M., & Persello, C. (2019). The Temporal Dynamics of Slums Employing a CNN-Based Change Detection Approach. *Remote Sensing*, *11*(23), 2844. https://doi.org/10.3390/rs11232844
Liu, T., Abd-Elrahman, A., Morton, J., & Wilhelm, V. L. (2018). Comparing fully convolutional networks, random forest, support vector machine, and patch-based deep convolutional neural networks for object-based wetland mapping using images from small unmanned aircraft system. *GIScience and Remote Sensing*, *55*(2), 243–264. https://doi.org/10.1080/15481603.2018.1426091
Mahabir, R., Stefanidis, A., Croitoru, A., Crooks, A., & Agouris, P. (2017). Authoritative and Volunteered Geographical Information in a Developing Country: A Comparative Case Study of Road Datasets in Nairobi, Kenya. *ISPRS International Journal of Geo-Information*, *6*(1), 24. https://doi.org/10.3390/ijgi6010024
Martin, H., Couclelis, H., & Clarke, K. C. (2005). The role of spatial metrics in the analysis and modeling of urban land use change. *Computers, Environment and Urban Systems*, *29*(4), 369–399. https://doi.org/10.1016/j.compenvurbsys.2003.12.001
Mboga, N., Georganos, S., Grippa, T., Lennert, M., Vanhuysse, S., & Wolff, E. (2019). Fully Convolutional Networks and Geographic Object-Based Image Analysis for the Classification of VHR Imagery. *Remote Sensing*, *11*(5), 597. https://doi.org/10.3390/rs11050597
McIver, D. K., & Friedl, M. A. (2002). Using prior probabilities in decision-tree classification of remotely sensed data. *Remote Sensing of Environment*, *81*(2–3), 253–261. https://doi.org/10.1016/S0034-4257(02)00003-2
Mubako, S., Belhaj, O., Heyman, J., Hargrove, W., Reyes, C., Mubako, S., … Reyes, C. (2018). Monitoring of Land Use/Land-Cover Changes in the Arid Transboundary Middle Rio Grande Basin Using Remote Sensing. *Remote Sensing*, *10*(12), 2005. https://doi.org/10.3390/rs10122005
Nielsen, M. A. (2015). Neural Networks and Deep Learning. Determination Press. Retrieved from http://neuralnetworksanddeeplearning.com/
Pal, M. (2008). Ensemble of support vector machines for land cover classification. *International Journal of Remote Sensing*, *29*(10), 3043–3049. https://doi.org/10.1080/01431160802007624

Parker, D. C., Evans, T., & Meretsky, V. (2001). *Measuring Emergent Properties of Agent-Based Landcover/Landuse Models using Spatial Metrics*. Paper presented at the 7th annual conference of the international society for computational economics. Retrieved from http://php.indiana.edu/dawparke/parker.pdf

Persello, C., & Stein, A. (2017). Deep Fully Convolutional Networks for the Detection of Informal Settlements in VHR Images. *IEEE Geoscience and Remote Sensing Letters*, *14*(12), 2325–2329. https://doi.org/10.1109/LGRS.2017.2763738

Pesaresi, M., Ehrlich, D., Ferri, S., Florczyk, A. J., Freire, S., Halkia, M., … Syrris, V. (2016). *Operating procedure for the production of the Global Human Settlement Layer from Landsat data of the epochs 1975, 1990, 2000, and 2014*. https://doi.org/10.2788/253582

Ramachandra, T. V., Aithal, B. H., & Sanna, D. D. (2012). Insights to urban dynamics through landscape spatial pattern analysis. *International Journal of Applied Earth Observation and Geoinformation*, *18*(1), 329–343. https://doi.org/10.1016/j.jag.2012.03.005

Ramachandra, T. V., Sellers, J. M., Bharath, H. A., & Vinay, S. (2019). Modeling urban dynamics along two major industrial corridors in India. *Spatial Information Research*, *27*(1), 37–48. https://doi.org/10.1007/s41324-018-0217-8

Reis, J. P., Silva, E. A., & Pinho, P. (2016). Spatial metrics to study urban patterns in growing and shrinking cities. *Urban Geography*, *37*(2), 246–271. https://doi.org/10.1080/02723638.2015.1096118

Rowley, H. V., Peters, G. M., Lundie, S., & Moore, S. J. (2012). Aggregating sustainability indicators: Beyond the weighted sum. *Journal of Environmental Management*, *111*, 24–33. https://doi.org/10.1016/j.jenvman.2012.05.004

Schiavina, M., Melchiorri, M., Corbane, C., Florczyk, A. J., Freire, S., Pesaresi, M., & Kemper, T. (2019). Multi-Scale Estimation of Land Use Efficiency (SDG 11.3.1) across 25 Years Using Global Open and Free Data. *Sustainability 2019, Vol. 11, Page 5674*, *11*(20), 5674. https://doi.org/10.3390/SU11205674

Seto, K. C., & Fragkias, M. (2005). Quantifying spatiotemporal patterns of urban land-use change in four cities of China with time series landscape metrics. *Landscape Ecology*, *20*(7), 871–888. https://doi.org/10.1007/s10980-005-5238-8

Srivastava, P. K., Han, D., Rico-Ramirez, M. A., Bray, M., & Islam, T. (2012). Selection of classification techniques for land use/land cover change investigation. *Advances in Space Research*, *50*(9), 1250-1265d. https://doi.org/10.1016/j.asr.2012.06.032

Srivastava, S. C. (1972). India Census In Perspective. *Census Library, India*. Retrieved from Registrar General & Census Commisssioner, India website: http://hdl.handle.net/123456789/371

Stefanov, W. L., Ramsey, M. S., & Christensen, P. R. (2001). Monitoring urban land cover change: An expert system approach to land cover classification of semiarid to arid urban centers. *Remote Sensing of Environment*, *77*(2), 173–185. https://doi.org/10.1016/S0034-4257(01)00204-8

Stevens, F. R., Gaughan, A. E., Linard, C., & Tatem, A. J. (2015). Disaggregating Census Data for Population Mapping Using Random Forests with Remotely-Sensed and Ancillary Data. *PLOS ONE*, *10*(2), e0107042. https://doi.org/10.1371/journal.pone.0107042

Tacoli, C., Gordon, M., & David, S. (2015). Urbanisation, rural-urban migration and urban poverty. *IIED*. Retrieved from http://pubs.iied.org/10725IIED

Tan, Y., Xiong, S., Li, Z., Tian, J., & Li, Y. (2019). Accurate detection of built-up areas from high-resolution remote sensing imagery using a fully convolutional network. *Photogrammetric Engineering and Remote Sensing*, *85*(10), 737–752. https://doi.org/10.14358/PERS.85.10.737

Taubenböck, H., Wegmann, M., Roth, A., Mehl, H., & Dech, S. (2009). Urbanization in India - Spatiotemporal analysis using remote sensing data. *Computers, Environment and Urban Systems*, *33*(3), 179–188. https://doi.org/10.1016/j.compenvurbsys.2008.09.003

Taubenböck, H., Wurm, M., Geiß, C., Dech, S., & Siedentop, S. (2019). Urbanization between

compactness and dispersion: designing a spatial model for measuring 2D binary settlement landscape configurations. *International Journal of Digital Earth*, *12*(6), 679–698. https://doi.org/10.1080/17538947.2018.1474957
Terfa, B. K., Chen, N., Liu, D., Zhang, X., & Niyogi, D. (2019). Urban expansion in Ethiopia from 1987 to 2017: Characteristics, spatial patterns, and driving forces. *Sustainability (Switzerland)*, *11*(10). https://doi.org/10.3390/su11102973
UN-Habitat. (2016). SDG indicators 11.3.1. Retrieved from https://unstats.un.org/sdgs/metadata/files/Metadata-11-03-01.pdf
United Nations. (2008). *Principles and Recommendations for Population and Housing Censuses Revision 2*. Retrieved from https://unstats.un.org/unsd/demographic/sources/census/docs/P&R_Rev2.pdf
United Nations. (2015). *Transforming our world: the 2030 Agenda for Sustainable Development.* Retrieved from https://www.un.org/ga/search/view_doc.asp?symbol=A/RES/70/1&Lang=E
United Nations. (2017). *United Nations Demographic Yearbook 2017*. https://doi.org/10.18356/50a88046-en-fr
United Nations. (2018). *The World's Cities in 2018*. Retrieved from https://www.flickr.com/photos/thisisin
Van Duijne, R. J. (2019). Why India's urbanization is hidden: Observations from "rural" Bihar. *World Development*, *123*, 104610. https://doi.org/10.1016/j.worlddev.2019.104610
Van Duijne, R. J., & Nijman, J. (2019). India's Emergent Urban Formations. *Annals of the American Association of Geographers*. https://doi.org/10.1080/24694452.2019.1587285
Volpi, M., & Tuia, D. (2017). Dense semantic labeling of subdecimeter resolution images with convolutional neural networks. *IEEE Transactions on Geoscience and Remote Sensing*, *55*(2), 881–893. https://doi.org/10.1109/TGRS.2016.2616585
Wang, S., Phillips, P., Sui, Y., Liu, B., Yang, M., & Cheng, H. (2018). Classification of Alzheimer's Disease Based on Eight-Layer Convolutional Neural Network with Leaky Rectified Linear Unit and Max Pooling. *Journal of Medical Systems*, *42*(5), 85. https://doi.org/10.1007/s10916-018-0932-7
Weber, E. M., Seaman, V. Y., Stewart, R. N., Bird, T. J., Tatem, A. J., McKee, J. J., … Reith, A. E. (2018). Census-independent population mapping in northern Nigeria. *Remote Sensing of Environment*, *204*, 786–798. https://doi.org/10.1016/j.rse.2017.09.024
Wilson, E. H., Hurd, J. D., Civco, D. L., Prisloe, M. P., & Arnold, C. (2003). Development of a geospatial model to quantify, describe and map urban growth. *Remote Sensing of Environment*, *86*(3), 275–285. https://doi.org/10.1016/S0034-4257(03)00074-9
Wirth, L. (1938). Urbanism as a way of life. *American Journal of Sociology*, *44*, 1–24. https://doi.org/10.1086/217913
World Bank. (2018). Population growth (annual %) - India | Data. Retrieved from https://data.worldbank.org/indicator/SP.POP.GROW?locations=IN
WorldPop. (2017). WorldPop - India 100m Population. Version 2.0. https://doi.org/10.5258/SOTON/WP00532
Wu, G., Guo, Y., Song, X., Guo, Z., Zhang, H., Shi, X., … Shao, X. (2019). A stacked fully convolutional networks with feature alignment framework for multi-label land-cover segmentation. *Remote Sensing*, *11*(9). https://doi.org/10.3390/rs11091051
Yang, L., Xian, G., Klaver, J. M., & Deal, B. (2003). Urban Land-Cover Change Detection through Sub-Pixel Imperviousness Mapping Using Remotely Sensed Data. *Photogrammetric Engineering & Remote Sensing*, *69*(9), 1003–1010. https://doi.org/10.14358/PERS.69.9.1003
Yang, Y., Zhuang, Y., Bi, F., Shi, H., & Xie, Y. (2017). M-FCN: Effective fully convolutional network-based airplane detection framework. *IEEE Geoscience and Remote Sensing Letters*, *14*(8), 1293–1297. https://doi.org/10.1109/LGRS.2017.2708722
Yoo, C., Han, D., Im, J., & Bechtel, B. (2019). Comparison between convolutional neural networks and random forest for local climate zone classification in mega urban areas using Landsat images. *ISPRS*

Journal of Photogrammetry and Remote Sensing, *157*, 155–170. https://doi.org/10.1016/j.isprsjprs.2019.09.009

Yu, F., & Koltun, V. (2016). *Multi-Scale Context Aggregation by Dilated Convolutions*. Paper presented at ICLR 2016. Retrieved from https://arxiv.org/abs/1511.07122

Zhang, C., Wei, S., Ji, S., & Lu, M. (2019). Detecting Large-Scale Urban Land Cover Changes from Very High Resolution Remote Sensing Images Using CNN-Based Classification. *ISPRS International Journal of Geo-Information*, *8*(4), 189. https://doi.org/10.3390/ijgi8040189

Zhang, P., Ke, Y., Zhang, Z., Wang, M., Li, P., & Zhang, S. (2018). Urban land use and land cover classification using novel deep learning models based on high spatial resolution satellite imagery. *Sensors (Switzerland)*, *18*(11). https://doi.org/10.3390/s18113717

Zhao, M., Zhou, Y., Li, X., Cao, W., He, C., Yu, B., … Zhou, C. (2019). Applications of Satellite Remote Sensing of Nighttime Light Observations: Advances, Challenges, and Perspectives. *Remote Sensing*, *11*(17), 1971. https://doi.org/10.3390/rs11171971

Zhou, Y., & Ma, L. (2005). China's urban population statistics: A critical evaluation. *Eurasian Geography and Economics*, *46*(4), 272–289. https://doi.org/10.2747/1538-7216.46.4.272

APPENDIX

Annex 1: Training and testing tiles for FCN in the Barharia cluster

	2005	2010	2018
Tile 1			
Tile 2			
Tile 3			
Tile 4			
Tile 5			

	2005	2010	2018
Tile 6			
Tile 7			
Tile 8			
Tile 9			
Tile 10			

	2005	2010	2018
Tile 11			
Tile 12			
Tile 13			

Annex 2: Classified maps for the Barharia cluster

	2005	2010	2018
Tile 1	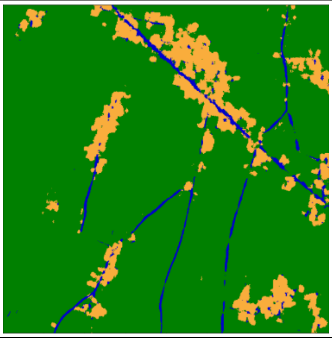	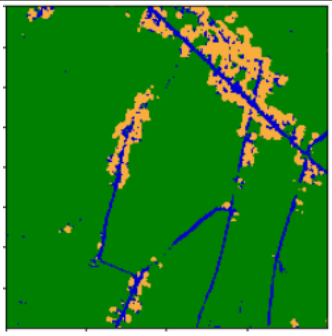	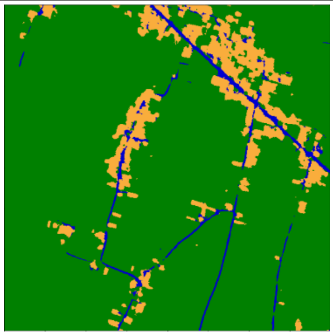
Tile 2	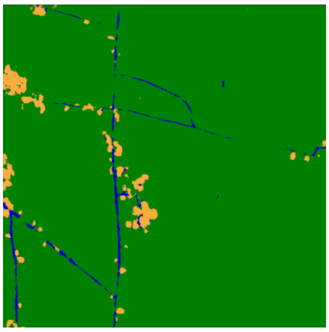	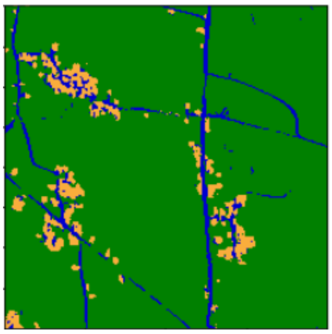	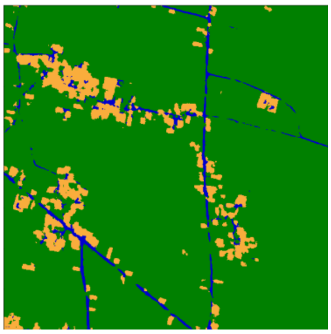
Tile 3	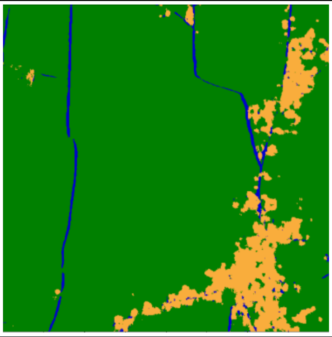	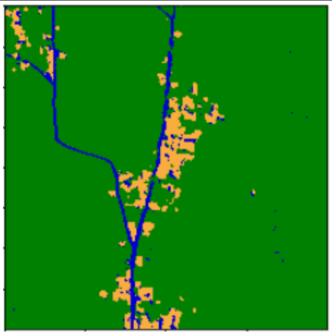	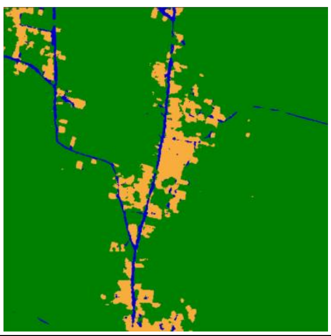
Tile 4	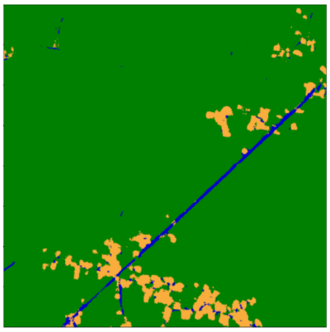	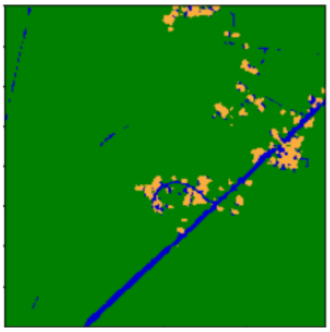	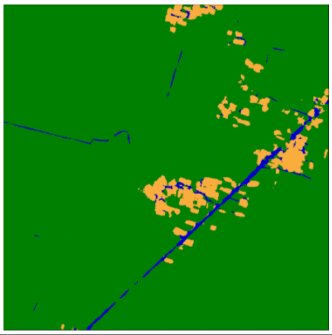
Tile 5	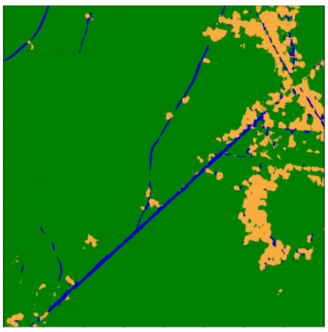	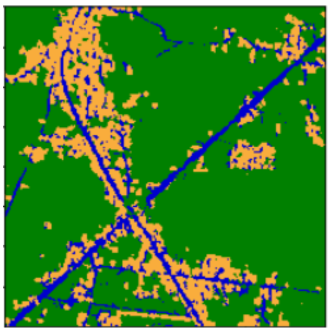	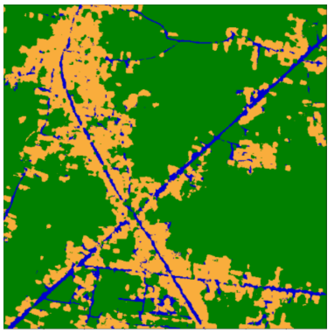
	2005	2010	2018

Tile 6	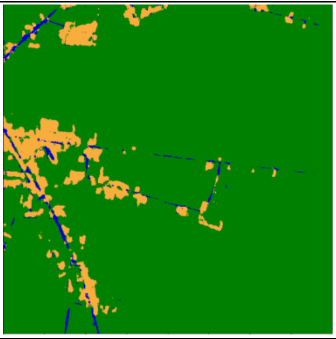	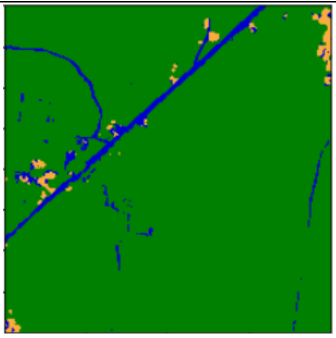	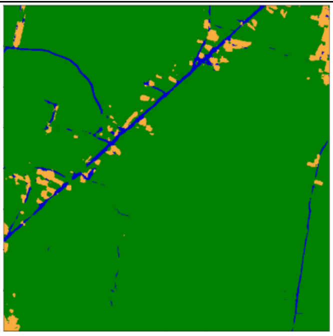
Tile 7	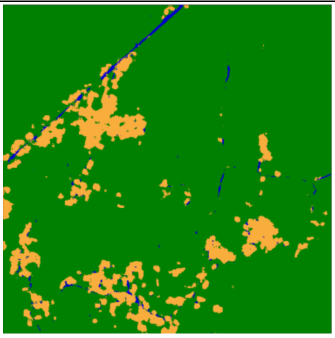	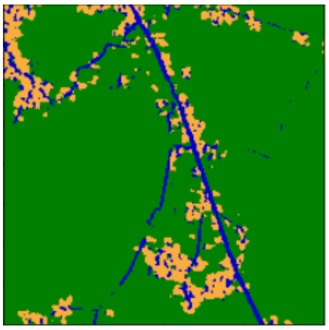	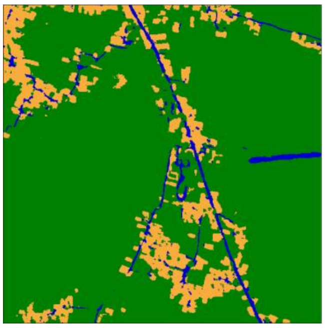
Tile 8	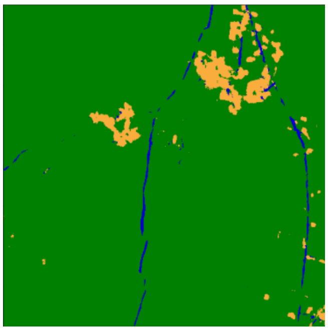	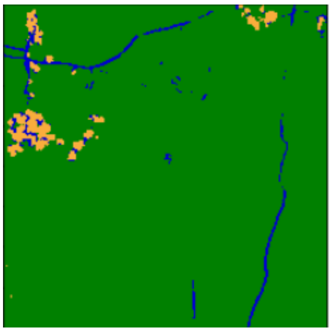	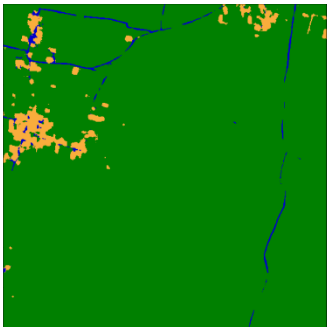
Tile 9	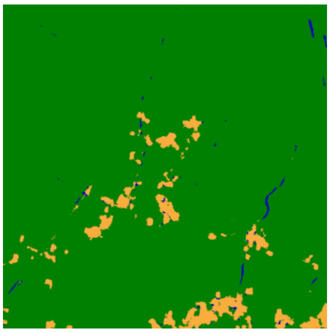	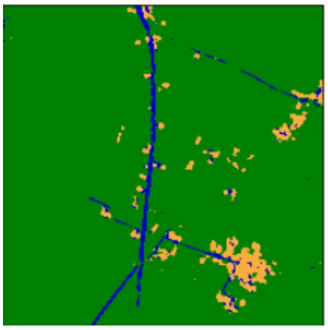	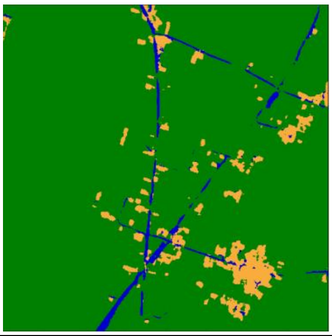
Tile 10	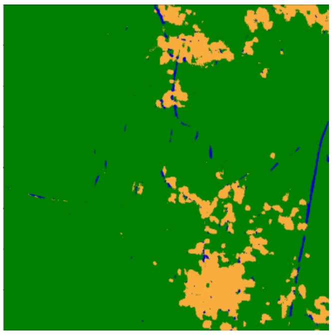	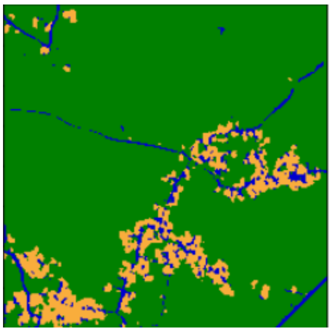	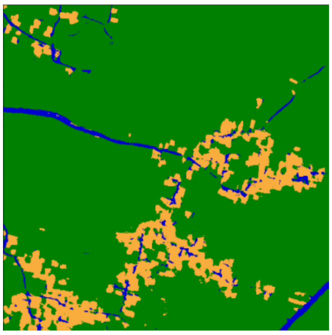

	2005	2010	2018
Tile 11	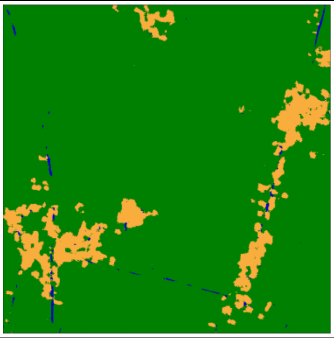	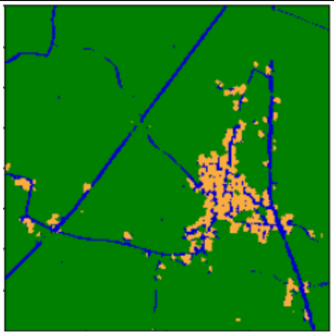	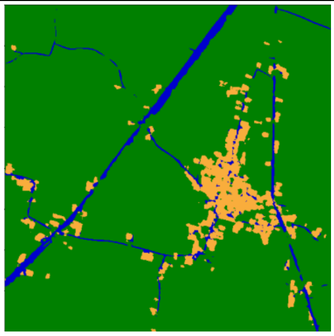
Tile 12		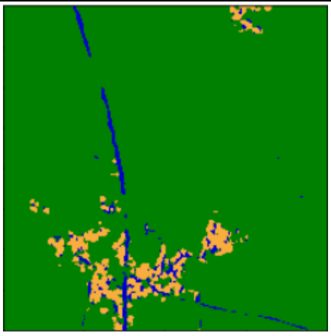	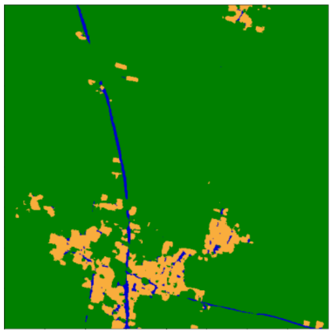
Tile13